

The SKIM-FA Kernel: High-Dimensional Variable Selection and Nonlinear Interaction Discovery in Linear Time

Raj Agrawal
Massachusetts Institute of Technology
and
Tamara Broderick
Massachusetts Institute of Technology

May 23, 2022

Abstract

Many scientific problems require identifying a small set of covariates that are associated with a target response and estimating their effects. Often, these effects are nonlinear and include interactions, so linear and additive methods can lead to poor estimation and variable selection. The Bayesian framework makes it straightforward to simultaneously express sparsity, nonlinearity, and interactions in a hierarchical model. But, as for the few other methods that handle this trifecta, inference is computationally intractable — with runtime at least quadratic in the number of covariates, and often worse. In the present work, we solve this computational bottleneck. We first show that suitable Bayesian models can be represented as Gaussian processes (GPs). We then demonstrate how a kernel trick can reduce computation with these GPs to $O(\# \text{ covariates})$ time for both variable selection and estimation. Our resulting fit corresponds to a sparse orthogonal decomposition of the regression function in a Hilbert space (i.e., a functional ANOVA decomposition), where interaction effects represent all variation that cannot be explained by lower-order effects. On a variety of synthetic and real datasets, our approach outperforms existing methods used for large, high-dimensional datasets while remaining competitive (or being orders of magnitude faster) in runtime.

Keywords: Hierarchical Bayesian modeling, Functional ANOVA, Gaussian processes, Kernel ridge regression, Reproducing kernel Hilbert spaces, Sparse high-dimensional regression

1 Introduction

Many scientific and decision-making tasks require learning complex relationships between a set of p covariates and target response from $N \ll p$ observed datapoints. For example, in genomics and precision medicine, researchers would like to identify a small set of genetic and environmental factors (out of potentially thousands or millions) associated with diseases and quantify their effects [Maher, 2008, Aschard, 2016, Slim et al., 2018, Greene et al., 2010]. Estimating these effects can be challenging, however, without sufficiently flexible models. Blood sugar levels, for example, could vary sinusoidally with the time of day (e.g., depending on when an individual has breakfast, lunch, and dinner). In other instances, effects can be challenging to estimate due to multiplicative interactions. A particular drug could help individuals with certain genetic characteristics but harm others. To learn such nuances in our data for better decision-making, we need statistical methods that can model nonlinear and interaction effects. We also need computationally efficient methods that can scale to large p settings. Unfortunately, as we detail below, existing methods suffer in at least one of these three categories.

Sparse linear regression methods (e.g., the Lasso) are typically fast but do not have the flexibility to learn nonlinear or interaction effects [Chen et al., 1998, Candes and Tao, 2007, Nakagawa et al., 2016]. SpAM extends the Lasso to model nonlinear effects but assumes additive effects [Liu et al., 2008]. Conversely, the hierarchical Lasso models interactions but assumes linearity, and its runtime scales quadratically with dimension [Bien et al., 2013]. Recently, Agrawal et al. [2019] developed a kernel trick to learn interactions in time linear in dimension, but this method assumes linear effects. Black-box models, such as neural networks and random forests, often include interactions and nonlinear effects for the sake of prediction. However, it is not clear how to actually access the effects from the fitted prediction model.

The *hierarchical functional ANOVA* [Stone, 1994], which includes many of the models described above as special cases, provides a powerful framework to jointly model interactions and nonlinear effects. Unfortunately, existing functional ANOVA methods, which are primarily kernel-regression based, do not scale well with dimension [Gu and Wahba, 1993, Lin and Zhang, 2006, Gunn and Kandola, 2004]; these methods use kernels that take $O(p^Q)$ time to evaluate, where Q equals the size of the highest order interaction. Hence, running kernel ridge regression for inference takes

$O(p^Q N^2 + N^3)$ time.

Contributions. We propose SKIM-FA kernels to model nonlinear and interaction effects. We show how to compute SKIM-FA kernels in $O(pQ)$ time by exploiting special low-dimensional structure. We motivate this structure from the perspective of hierarchical Bayesian modeling. Then, we use equivalences between kernel ridge regression, Gaussian processes, and conjugate Bayesian linear regression to develop our efficient inference procedure.

Outline. We start by describing how to model nonlinear interaction effects and encode sparsity using hierarchical Bayesian modeling in Section 2. In Section 3, we develop two kernel tricks to perform inference more efficiently when the covariates are independent. Then, we extend our procedure to the general covariate case in Section 4. We defer implementation details of our final algorithm to Section 5. We conclude by discussing related work in Section 6 and benchmarking our method against other methods often used to model high-dimensional data in Section 7.

2 A framework for non-linear interactions and sparsity

2.1 Problem Statement

Suppose we collect data $D = \{(x^{(n)}, y^{(n)})\}_{n=1}^N$ with covariates $x^{(n)} \in \mathbb{R}^p$ and continuous scalar responses $y^{(n)}$. We model $y^{(n)} = f^*(x^{(n)}) + \epsilon^{(n)}$, where $\epsilon^{(n)} \stackrel{\text{iid}}{\sim} \mathcal{N}(0, \sigma_{\text{noise}}^2)$, $x^{(n)} \stackrel{\text{iid}}{\sim} \mu$, and the unknown regression function f^* belongs to some class of functions \mathcal{H} . Using only noisy realizations of f^* , we would like to identify what covariates f^* depends on (i.e., perform variable selection) and recover interactions effects. To that end, we use penalized regression:

$$\hat{f} = \arg \min_{f \in \mathcal{H}} \sum_{n=1}^N \mathcal{L}(y^{(n)}, f(x^{(n)})) + J(f), \quad (1)$$

where $\mathcal{L}(\cdot, \cdot)$ and $J(f)$ denote some loss function and penalty on model complexity, respectively. This paper focuses on four subproblems resulting from Eq. (1): (P1) picking \mathcal{H} to model interactions, (P2) selecting $\mathcal{L}(\cdot, \cdot)$ and $J(f)$ to induce sparsity, (P3) tractably solving Eq. (1) for our choice of sparsity-inducing $J(f)$, and (P4) efficiently reporting effects in \hat{f} .

2.2 Our contributions: an overview

We describe, at a high level, our solutions to subproblems P1 through P4, and what parts of our solutions are new. Our solutions to P3 and P4 are our core contributions.

P1: Constructing \mathcal{H} . Our construction of \mathcal{H} in Section 2.3 is based on Huang [1998]. We use the hierarchical functional ANOVA introduced in Stone [1994] to make recovering interaction effects a well-defined inference task (i.e., statistically identifiable).

P2: Selecting the loss and penalty. We select the loss and penalty from a hierarchical Bayesian modeling point-of-view in Section 2.4. In particular, we choose the loss \mathcal{L} to correspond to a negative log-likelihood of the data and the penalty $J(f)$ to correspond to a negative log prior of f . Existing sparse Bayesian interaction methods do not work at our level of generality. Nevertheless, our proposed class of priors is heavily influenced by existing sparse Bayesian interaction models.

P3: Solving Eq. (1). We solve Eq. (1) in time linear in p by using two kernel tricks to (1) reduce the cost of modeling nonlinear functions and (2) avoid summing over a combinatorial number of interaction terms. The first kernel trick, described in Section 3, is based on the foundational smoothing spline ANOVA (SS-ANOVA) work by Gu and Wahba [1993]. To make the connection to SS-ANOVA, we show that there exists a duality between our class of hierarchical models (see P2) and reproducing kernel Hilbert spaces induced by what we call *model selection kernels*. Our model selection kernels generalize the kernels used in Gu and Wahba [1993] by removing the requirement that all covariates be independent. Our second kernel trick, which allows us to avoid summing over a combinatorial number of interaction terms, applies to a subset of model selection kernels. We call this subset of kernels *SKIM-FA* kernels and prove that SKIM-FA kernels have desirable statistical properties from the hierarchical Bayesian modeling point-of-view.

P4: Reporting effects. For the case of independent covariates, we report effects using the procedure in Gu and Wahba [1993]. Our new contribution, provided in Section 4, is developing an efficient algorithm to report effects for the non-independent case.

2.3 Interactions and identifiability for nonlinear functions

We construct \mathcal{H} in Eq. (1) by considering functions on \mathbb{R}^p that can be written as a sum of lower-dimensional functions (i.e., interaction effects) that depend on at most $Q < p$ covariates. Our goal is to estimate these interaction effects. Unfortunately, as we detail below, such an expansion is not unique, and therefore not a valid target of inference. To make inference over \mathcal{H} well-defined, we use the *hierarchical functional ANOVA* [Stone, 1994].

Modeling Interactions. Let $\mathcal{H} = \mathcal{H}_Q := \bigoplus_{V:|V|\leq Q} \mathcal{H}_V$, where \mathcal{H}_V belongs to the space of all square-integrable functions of x_V (with respect to the probability measure μ) and $V \subset [p] := \{1, \dots, p\}$. Then,

$$\begin{aligned} \bigoplus_{V:|V|\leq Q} \mathcal{H}_V &= \left\{ f : f = \sum_{V:|V|\leq Q} f_V(x_V), f_V \in \mathcal{H}_V \right\} \\ &= \left\{ f : f = f_\emptyset + \sum_{i=1}^p f_{\{i\}}(x_i) + \sum_{i<j}^p f_{\{i,j\}}(x_i, x_j) + \dots + \sum_{V:|V|=Q}^p f_V(x_V) \right\}, \end{aligned} \quad (2)$$

where f_\emptyset belongs to the space of constant functions $\mathcal{H}_\emptyset = \{\theta : \theta \in \mathbb{R}\}$. Similar to additive models, $f_{\{i\}}(x_i)$ has the interpretation as the main or marginal effect of covariate x_i on y . Similarly, $f_{\{i,j\}}(x_i, x_j)$ has the interpretation as the two-way or pairwise effect of x_i and x_j on y . Unfortunately, the components in Eq. (2) are not identifiable without further constraints. For example, if $f^*(x) = f_{\{1\}}(x_1) + f_{\{2\}}(x_2) + f_{\{1,2\}}(x_1, x_2)$, then f^* also decomposes as $f_{\{1\}}(x_1) + [f_{\{2\}}(x_2) + 5] + [f_{\{1,2\}}(x_1, x_2) - 5]$.

Identifiability with the Functional ANOVA. To resolve identifiability issues, we construct a smaller space of functions $\mathcal{H}_V^o \subset \mathcal{H}_V$, where \mathcal{H}_V^o includes only functions whose variation cannot be explained by lower-order effects of x_V :

$$\mathcal{H}_V^o = \{f_V \in \mathcal{H}_V : \forall A \subsetneq V, \forall f_A \in \mathcal{H}_A, \langle f_V, f_A \rangle_\mu = 0\}, \quad (3)$$

where $\langle \cdot, \cdot \rangle_\mu$ is an inner product on L^2 . That is, for $f_A \in \mathcal{H}_A$ and $f_B \in \mathcal{H}_B$, $\langle f_A, f_B \rangle_\mu = \mathbb{E}_{x \sim \mu}[f_A(x_A)f_B(x_B)]$.

Theorem 2.1. [Stone, 1994, Huang, 1998] Suppose $f \in \mathcal{H}_Q$ and μ is absolutely continuous with respect to Lebesgue measure. Further, suppose that the domain of functions in \mathcal{H}_Q range over a compact set \mathcal{X} of \mathbb{R}^p . Then, there exist (μ -almost everywhere) unique functions $f_V \in \mathcal{H}_V^o$ such that $f = \sum_{V:|V|\leq Q} f_V$.

Definition 2.2. Suppose $f = \sum_{V:|V|\leq Q} f_V$ where $f_V \in \mathcal{H}_V^o$. Then, $\sum_{V:|V|\leq Q} f_V$ is called the *functional ANOVA decomposition* of f with respect to μ .

In light of Theorem 2.1, we assume compactness throughout to have a well-defined target of inference (i.e., the functional ANOVA decomposition of f in Definition 2.2). By the orthogonality constraints in Eq. (3), the effect $f_{\{i,j\}}(x_i, x_j)$ in Definition 2.2 represents, for example, the variation that cannot be explained by 1D functions of x_i and x_j and an intercept. When the covariates are independent, then the signal variance further decomposes as

$$\text{var}(f) = \text{var}(f_{\{\emptyset\}}) + \sum_i \text{var}(f_{\{i\}}) + \sum_{i,j} \text{var}(f_{\{i,j\}}) + \cdots \text{var}(f_{\{1,2,\dots,p\}}(x_1, \dots, x_p)), \quad (4)$$

where $\text{var}(f) = \langle f, f \rangle_\mu$. Hence, Eq. (4) allows us to *analyze* how the *variance* of the *function* is distributed across the interactions of different orders. Hence, the name functional analysis of variance or ANOVA.

2.4 How to achieve sparsity for nonlinear functions

To complete our specification of Eq. (1), we still need to pick a loss and penalty function on \mathcal{H}_Q . We motivate our choice of loss and penalty from a Bayesian point-of-view. That is, we view $\mathcal{L}(\cdot, \cdot)$ as the negative log-likelihood function, $J(f)$ as the negative log prior on f , and \hat{f} as the maximum a priori (MAP) estimate under our proposed Bayesian model.

Our Loss. Since the noise terms are Gaussian (Section 2.1), the negative log-likelihood is quadratic: $\mathcal{L}(y, f(x)) = (y - f(x))^2$ (i.e., squared-error loss).

Our Penalty. Since we are primarily interested in the case when f^* is sparse, i.e., when many of the effects f_V equal zero, we would like $J(f)$ to promote sparsity. To this end, we take a basis

expansion of each component space, and then place a sparsity prior on the basis coefficients to construct $J(f)$. We assume that for all $V \subset [p]$ and $1 \leq |V| \leq Q$, there exists a $B_V \in \mathbb{N} \cup \{\infty\}$ and feature map $\Phi_V : \mathbb{R}^{|V|} \mapsto \mathbb{R}^{B_V}$ such that the components of Φ_V form a basis of \mathcal{H}_V^o . Then, for any $f_V \in \mathcal{H}_V^o$, there exists $\Theta_V \in \mathbb{R}^{B_V}$ such that $f_V(x_V) = \Theta_V^T \Phi_V(x_V)$. Hence, if we can estimate Θ_V , we can estimate the functional ANOVA decomposition of f^* by Theorem 2.1.

To obtain a MAP estimate of Θ_V , we draw each $\Theta_V \sim \mathcal{N}(0, \theta_V \cdot I_{B_V} \times I_{B_V})$, where θ_V is a non-negative auxiliary parameter drawn from a sparsity prior (e.g., a Laplace prior); see Section 5 for our particular choice of sparsity prior. If $\theta := \{\theta_V\}$ is sparse, then we claim that $\{f_V\}$ is sparse. To understand why, suppose $\theta_V = 0$. Then, the prior variance of f_V equals 0. Hence, f_V will equal 0.

Since Φ_V is a basis of \mathcal{H}_V^o and our prior on Θ_V has full support on \mathbb{R}^{B_V} , our choice of likelihood and prior allows us to model any $f \in \mathcal{H}_Q$. We summarize our hierarchical Bayesian model below:

$$\begin{aligned} \Theta_V \mid \theta_V &\sim \mathcal{N}(0, \theta_V \cdot I_{B_V} \times I_{B_V}), \quad V \subset [p], \quad |V| \leq Q, \quad \theta_V \geq 0 \\ f &= \sum_{V: |V| \leq Q} \Theta_V^T \Phi_V(\cdot) \\ y^{(n)} \mid x^{(n)}, \Theta, \sigma_{\text{noise}}^2 &\sim \mathcal{N}(f(x^{(n)}), \sigma_{\text{noise}}^2), \quad n \in [N], \end{aligned} \tag{5}$$

where the likelihood in the first equation corresponds to $\exp(-J(f))$ and the likelihood in the last equation corresponds to $\exp(-\mathcal{L}(y^{(n)}, f(x^{(n)})))$. While other likelihoods and priors exist to model interactions and sparsity, many existing sparse Bayesian methods are instantiations of Eq. (5), and have desirable statistical properties; see, for example, Wei et al. [2019], Curtis et al. [2014], Griffin and Brown [2017], Agrawal et al. [2019], Chipman [1996], George and McCulloch [1993]. In the next section, we exploit the special Gaussian and interaction structure in Eq. (5) for faster inference.

3 Using two kernel tricks to reduce computation cost

In principle, we can analytically compute the MAP estimate of Θ_V in Eq. (5) (and hence solve Eq. (1) in closed-form); conditional on θ , Eq. (5) reduces to conjugate Bayesian regression.

Unfortunately, unless p is very small or $Q = 1$, computing this closed-form solution is typically computationally intractable, for reasons we describe next. To remedy this computational intractability, we show how to make inference scale linearly with p by exploiting special model structure in Section 3.1 and Section 3.2.

Intractability of Conjugate Bayesian Regression. Our model in Eq. (5) has $B_Q := \sum_{V:|V|\leq Q} B_V$ parameters. In general, computing the MAP estimate of these B_Q parameters requires inverting a $B_Q \times B_Q$ covariance matrix [Rasmussen and Williams, 2006, Chapter 2]. Hence, the computational cost of MAP inference scales as $O(B_Q^3 + NB_Q^2)$. B_Q may be prohibitively large for two reasons. The first problem arises if any of the basis expansion sizes (i.e., a particular B_V) is large. If \mathcal{H}_V^o is infinite-dimensional, for example, then $B_V = \infty$. Even if all the \mathcal{H}_V^o are finite-dimensional, B_V typically grows exponentially with the size of $|V|$; see, for example, Huang [1998]. The second issue arises from the combinatorial sum over interactions; even if all of the B_V equal 1, B_Q still has on the order of $O(p^Q)$ terms. Hence, without additional structure, the computation time for conjugate Bayesian regression is lower bounded by $\Omega(p^{3Q} + p^{2Q}N)$. Fortunately, due to unique structure in our problem, we show how to avoid the cost of explicitly generating the basis expansion (“Trick one” in Section 3.1), and summing over all $O(p^Q)$ interactions (“Trick two” in Section 3.2).

In what follows, we assume θ is fixed. Then, we show how to estimate θ in Section 5.

3.1 Trick one: How to represent and access sparsity without incurring the cost of a basis expansion

We show how to remove the computational dependence on the size of B_V through a kernel trick. Our kernel generalizes the one used in Gu and Wahba [1993], which assumes independent covariates, to the case of general covariate distributions. In order to prove the existence of a kernel trick, we make the following assumption:

Assumption 3.1. Each \mathcal{H}_V is a reproducing kernel Hilbert space (RKHS).

Given that there exists reproducing kernels that can approximate any continuous function

arbitrarily well, Assumption 3.1 is a mild condition [Micchelli et al., 2006]. The non-trivial part is proving the existence of a kernel to induce \mathcal{H}_V^o , which is not immediate due to the orthogonality constraints in Eq. (3).

Proposition 3.2. *(existence of a kernel trick) Under Assumption 3.1, there exists a positive-definite kernel k_V such that $k_V(x, \tilde{x}) = \langle \Phi_V(x), \Phi_V(\tilde{x}) \rangle$, where the components of $\Phi_V \in \mathbb{R}^{B_V}$ form a countable basis of \mathcal{H}_V^o .*

We prove Proposition 3.2 in Appendix A.1. In Section 3.2, we show how to efficiently evaluate k_V without explicitly computing the feature maps. In light of Proposition 3.2, we introduce *model selection kernels* to rewrite the model in Eq. (5) as a Gaussian process. We then show how this reparametrization allows us to perform inference more efficiently.

Definition 3.3. A kernel k_θ is a *model selection kernel* if it can be written as $\sum_{V:|V|\leq Q} \theta_V k_V$, where k_V is the reproducing kernel for \mathcal{H}_V^o and $k_\emptyset(x, \tilde{x}) = 1$ (i.e., the kernel k_\emptyset induces the space of constant functions \mathcal{H}_\emptyset).

Lemma 3.4. *Suppose k_θ is a model selection kernel. Then, the distribution of $y^{(n)} \mid x^{(n)}$ in Eq. (5) has the same distribution as instead placing a zero-mean Gaussian process prior with covariance kernel k_θ on f .*

Based on the reparametrization in Lemma 3.4 (see Appendix A.4 for the proof), $J(f)$ equals the penalty induced by the kernel k_θ . Hence, the solution to Eq. (1) reduces to kernel ridge regression (or equivalently equals the posterior predictive mean of the Gaussian process) by Rasmussen and Williams [2006, Chapter 2]:

$$\hat{f}(x) = \bar{f}_\theta(x) := \sum_{n=1}^N \hat{\alpha}_n k_\theta(x_n, x), \quad \hat{\alpha} = (K_\theta + \sigma_{\text{noise}}^2 I_{N \times N})^{-1} Y, \quad (6)$$

where $Y_n = y^{(n)}$ and $[K_\theta]_{nm} = k_\theta(x^{(n)}, x^{(m)})$.

Unlike the “weight-space view” in Section 2.4 where $f_V = \Theta_V^T \Phi_V(\cdot)$, it is not clear how to actually recover the effects f_V from the prediction function \bar{f}_θ . For general kernels, accessing f_V (and consequently computing the functional ANOVA of \bar{f}_θ) lacks an analytical form. Fortunately, we can easily recover f_V from \bar{f}_θ for model selection kernels:

Lemma 3.5. Suppose k_θ is a model selection kernel and $f^{(M)}(x) = \sum_{m=1}^M \alpha_m k_\theta(x_m, x)$ for $\alpha_m \in \mathbb{R}$ and $x_m \in \mathbb{R}^p$. Then, $f^{(M)}(x) = \sum_{V: |V| \leq Q} f_V$, where $f_V = \theta_V \sum_{m=1}^M \alpha_m k_V(x_m, x) \in \mathcal{H}_V^o$.

As a consequence of Lemma 3.5, model selection kernels make it easy to perform variable selection¹ as well.

Corollary 3.6. (nonlinear variable selection) Suppose $f^{(M)}(x) = \sum_{m=1}^M \alpha_m k_\theta(x_m, x)$. Then, $f^{(M)}(x)$ functionally depends on the set of covariates $\{i : \exists V \subset [p], i \in V \text{ s.t. } \theta_V \neq 0\}$.

While we have avoided the cost of generating the basis expansion to solve Eq. (1), computing Eq. (6) is still computationally intractable; k_θ sums over $O(p^Q)$ kernels. Hence, the cost to compute the kernel matrix K_θ and invert $(K_\theta + \lambda I_{N \times N})$ takes $O(N^2 p^Q)$ and $O(N^3)$ time, respectively.

3.2 Trick two: A recursion to avoid a combinatorially large summation over interactions in the presence of covariate independence

We show how to compute k_θ in $O(pQ)$ time (and hence solve Eq. (6) in $O(pQN^2 + N^3)$ time) for a particular subset of model selection kernels that we call *SKIM-FA* kernels. In what follows, we start by motivating SKIM-FA kernels from the hierarchical Bayesian characterization of model selection kernels in Eq. (5). Then, we show when the covariates are independent, we can compute SKIM-FA kernels much more efficiently using a second kernel trick. In Section 4, we generalize to the non-independent covariate case by building on the procedure described in this section.

The Sparse Kernel Interaction Model for Functional ANOVA (SKIM-FA). In Eq. (5), $\{\theta_V\}$ does not necessarily have any special structure. SKIM-FA, on the other hand, assumes a low-rank factorization structure, namely that $\theta_V = \prod_{i \in V} \eta_{|V|}^2 \kappa_i^2$ for some non-negative random

¹For general nonlinear regression functions, performing variable selection can be challenging; in principle, showing that a fitted regression function does not depend on x_i requires checking that the fitted function is constant in x_i across the entire domain.

vectors $\kappa \in \mathbb{R}_+^p$ and $\eta \in \mathbb{R}_+^{Q+1}$. Then, the prior on Θ_V in Eq. (5) simplifies to

$$\Theta_V \mid \eta, \kappa \sim \mathcal{N} \left(0, \eta_{|V|}^2 \prod_{i \in V} \kappa_i^2 \cdot I_{B_V} \times I_{B_V} \right), \quad (7)$$

for SKIM-FA, which generalizes the prior used in Agrawal et al. [2019] for linear pairwise interaction models.

SKIM-FA Interpretation. In Eq. (7), $\eta_{|V|}^2$ quantifies the overall strength of $|V|$ -way interactions by modifying the prior variance of all effects of order $|V|$. κ_i plays the role of a “variable importance” measure for covariate x_i by affecting the prior variance of all effects involving covariate x_i . Hence, if it turns out an effect involving x_i is strong, the posterior of κ_i will place high probability at large values (i.e., indicating that covariate x_i has high “importance”). Notice that if $\kappa_i = 0$, then the prior variance of Θ_V equals 0 whenever $i \in V$. Consequently, all effects involving x_i will equal 0. Hence, we can perform variable selection in $O(p)$ time by just examining the sparsity pattern of κ instead of in $O(p^Q)$ time using Corollary 3.6. In Section 5, we show how we select our sparsity prior on κ . Finally, note that while we added more structure to the prior, we have not lost modeling flexibility; as long as $\mathbb{P}(\kappa_i)$ does not equal 0 with probability one, then the prior variance of Θ_V will be non-zero. Hence, our prior will have support on all of \mathcal{H}_Q .

Definition 3.7. A *SKIM-FA kernel* is a model selection kernel that can be written as

$$k_{\text{SKIM-FA}}(x, \tilde{x}) = \sum_{V: |V| \leq Q} \left[\eta_{|V|}^2 \prod_{i \in V} \kappa_i^2 \right] k_V(x, \tilde{x}).$$

for some $\kappa \in \mathbb{R}^p$ and $\eta \in \mathbb{R}^{Q+1}$.

Proposition 3.8. For a SKIM-FA kernel, Eq. (5) can be replaced by Eq. (7) in Lemma 3.4.

Proof. Set $\theta_V = \eta_{|V|}^2 \prod_{i \in V} \kappa_i^2$ in Lemma 3.4. □

Efficient Evaluation of SKIM-FA Kernels. Recall that k_i is the reproducing kernel for \mathcal{H}_i^o . Suppose, for the moment, that the reproducing kernel k_V for \mathcal{H}_V^o equals $\prod_{i \in V} k_i$ (we will shortly show that this condition holds when the covariates are independent). Then, by Theorem 3.9 and Corollary 3.10 below, we can compute SKIM-FA kernels orders of magnitude faster by not explicitly summing over all $O(p^Q)$ interactions in Definition 3.7.

Theorem 3.9. Suppose $k_V(x, \tilde{x}) = \prod_{i \in V} k_i(x_i, \tilde{x}_i)$. Then,

$$\begin{aligned} k_{\text{SKIM-FA}}(x, \tilde{x}) &= \sum_{q=1}^Q \eta_q^2 \bar{k}_q(x, \tilde{x}) \quad \text{s.t.} \\ \bar{k}_q(x, \tilde{x}) &= \frac{1}{q} \sum_{s=1}^q (-1)^{s+1} \bar{k}_{q-s}(x, \tilde{x}) k^s(x, \tilde{x}), \quad \bar{k}_0(x, \tilde{x}) = 1, \\ k^s(x, \tilde{x}) &= \sum_{i=1}^p \kappa_i^{2s} [k_i(x_i, \tilde{x}_i)]^s. \end{aligned} \tag{8}$$

As we show in Appendix A.5, the key to proving Theorem 3.9 is an old recursive kernel formula provided in Vapnik [1995, pg. 199]. From Theorem 3.9, we have two corollaries. The first requires a short inductive argument; see Appendix A. The second follows immediately by setting $Q = 2$ into Eq. (8).

Corollary 3.10. $k_{\text{SKIM-FA}}(x, \tilde{x})$ takes $O(pQ)$ time to evaluate on a pair of points.

Corollary 3.11. Suppose $Q = 2$. Then, $k_{\text{SKIM-FA}}(x, \tilde{x})$ equals

$$0.5\eta_2^2 \left[\left(\sum_{i=1}^p \kappa_i^2 k_i(x_i, \tilde{x}_i) \right)^2 - \sum_{i=1}^p \kappa_i^4 [k_i(x_i, \tilde{x}_i)]^2 \right] + \eta_1^2 \sum_{i=1}^p \kappa_i^2 k_i(x_i, \tilde{x}_i) + \eta_0^2. \tag{9}$$

To see why “kernel trick two” in Eq. (8) indeed acts as another kernel trick, consider the linear interaction case when \mathcal{H}_Q consists of interactions of the form $\prod_{i \in V} x_i$. Suppose further that κ and η are equal to the ones vector. Then, $k_{\text{SKIM-FA}}(x, \tilde{x}) = \sum_{V: |V| \leq Q} \prod_{i \in V} x_i \tilde{x}_i$, which explicitly generates and sums over the interactions $\prod_{i \in V} x_i$. However, it is well known that polynomial kernels implicitly generate interactions, and hence can be used instead to avoid summing over all interactions. The core idea in Eq. (8) is similar; the kernels k^s raised to the s power in Eq. (8) implicitly generate interactions of order equal to s just like a polynomial kernel. However, instead of generating interactions of the form $\prod_{i \in V} x_i$, k^s operates on one-dimensional kernels k_i to generate interactions of the form $\prod_{i \in V} k_i$. Since $k_V = \prod_{i \in V} k_i$ by assumption, these “interactions” of kernels span \mathcal{H}_V^o by the product property of kernels.

To understand when $k_V = \prod_{i \in V} k_i$ in Theorem 3.9 actually holds, we provide sufficient conditions based a result from Gu and Wahba [1993]. We leave our construction of k_i to Appendix C.

Assumption 3.12. (Tensor product space) For all $V \subset [p]$ and $1 \leq |V| \leq Q$, $\mathcal{H}_V = \bigotimes_{i \in V} \mathcal{H}_i$.

Proposition 3.13. [Gu and Wahba, 1993] Suppose $\mu = \mu_{\otimes}$, where $\mu_{\otimes}(x) := \mu_1(x_1) \otimes \mu_2(x_2) \cdots \otimes \mu_p(x_p)$ and μ_j is the marginal distribution of x_j . Then, under Assumption 3.1 and Assumption 3.12, $k_V = \prod_{i \in V} k_i$.

Since any Hilbert space of square-integrable functions of x_V can be approximated arbitrarily well by taking tensor products of one-dimensional Hilbert spaces by Stone [1994], Huang [1998], Assumption 3.12 is a mild assumption. The more problematic assumption is that all covariates are independent (i.e., that $\mu = \mu_{\otimes}$).

4 How to get sparsity, interactions, and fast inference when covariates are dependent

Here we extend to the general μ case. We start by motivating why this extension is important in Section 4.1. Then, in Section 4.2, we develop a change-of-basis formula to take the functional ANOVA decomposition of \bar{f}_{θ} with respect to μ_{\otimes} to one with respect to μ . While our formula assumes $Q = 2$, we expect that our formula naturally extends beyond the pairwise case.

4.1 Practical problems that arise when assuming independent covariates

Since $\mu_{\otimes} = \mu_1(x_1) \otimes \mu_2(x_2) \cdots \otimes \mu_p(x_p)$, μ_{\otimes} has the same 1D marginal distributions as μ . Nevertheless, we prove that the functional ANOVA decomposition of an $f \in \mathcal{H}$ can be *arbitrarily* different depending on if μ_{\otimes} or μ is selected. We prove this claim by showing something stronger, namely that the intercepts between two functional ANOVA decompositions can be arbitrarily far apart (see Appendix A.3 for the proof of Proposition 4.1).

Proposition 4.1. For any $\Delta > 0$, there exists a probability measure μ and square-integrable f such that the relative difference

$$\frac{|f_{\emptyset}^{\mu} - f_{\emptyset}^{\mu_{\otimes}}|}{|f_{\emptyset}^{\mu}|} > \Delta, \quad \text{where} \quad f_{\emptyset}^{\mu} = \mathbb{E}_{\mu} f(X) \quad \text{and} \quad f_{\emptyset}^{\mu_{\otimes}} = \mathbb{E}_{\mu_{\otimes}} f(X).$$

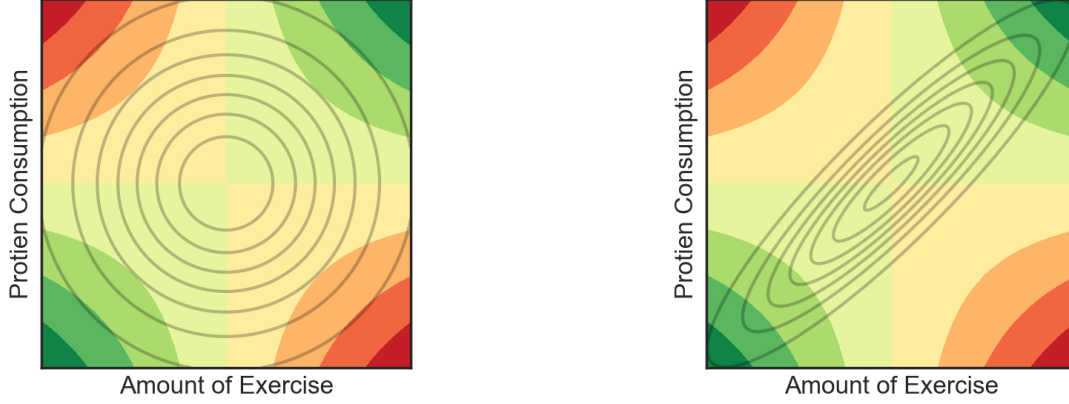


Figure 1: The colors denote the contour plot of the function $f^*(x_1, x_2) = 100x_1x_2 - 50$. Darker green indicates larger positive values while darker red indicates larger negative values. The gray solid lines in the left and right hand figures represent the density contours of μ_{\otimes} and μ in Example 4.2, respectively.

To build intuition for Proposition 4.1, and motivate using μ instead of μ_{\otimes} to compute the functional ANOVA decomposition of \bar{f}_{θ} , consider the following toy example.

Example 4.2. Suppose $f^*(x_1, x_2) = 100x_1x_2 - 50$, where x_1 could represent exercise, x_2 protein consumption, and $f^*(x_1, x_2)$ the expected percent decrease in body mass index after taking a weight-loss drug for an individual who consumes x_1 grams of protein and exercises x_2 times per week. Suppose exercise and protein consumption are positively correlated and that μ corresponds to a multivariate Gaussian distribution with mean zero, unit covariance, and correlation equal to 0.9. Then, μ_{\otimes} corresponds to a multivariate Gaussian distribution with mean zero, unit covariance but correlation equal to 0. Suppose we report the intercept f_{\emptyset} to summarize the typical decrease in body mass index in a population of people who might take the weight-loss drug (e.g., after drug approval). In the functional ANOVA decomposition of f^* with respect to μ , $f_{\emptyset} = \mathbb{E}_{\mu}[f^*] = \mathbb{E}_{\mu}[f^* + \epsilon] = \mathbb{E}_{\mu}[y] \approx 39$. Hence, this intercept says that, on average, people in this population should decrease their body mass index by 39% if they take the drug. If we instead use μ_{\otimes} , then $f_{\emptyset} = \mathbb{E}_{\mu_{\otimes}}[f^*] = -50 \neq \mathbb{E}_{\mu}[f^*]$, suggesting that the drug *increases* body mass index.

In the μ_\otimes case, it is not clear how to interpret the intercept; μ_\otimes averages the regression surface f^* over individuals who rarely occur in the actual population (e.g., those who exercise very frequently but do not consume much protein); see also Section 4.1 for a visualization.

4.2 A change of basis to handle covariate dependence

We generalize to the non-independent case through a change-of-basis formula provided in Theorem 4.5. Our formula allows us to re-express the effects estimated using the kernel in Section 3.2, which assumes independent covariates, to one with respect to the actual distribution μ . Our idea is similar to ideas in numerical linear algebra; we use one parameterization of a vector space, in our case the space of functions \mathcal{H}_Q , that makes computation “nice.” Once we finish computation in the “nice” parameterization, we use a change-of-basis formula to report the actual quantity we care about in the original parameterization of the space, namely reporting the functional ANOVA decomposition of our fit \bar{f}_θ with respect to μ .

To make this idea mathematically precise, suppose we can write \mathcal{H}_Q using two different parameterizations, one that uses μ_\otimes in Eq. (3) (denoted as $\mathcal{H}_{V,\mu_\otimes}^o$) and the other that uses μ in Eq. (3) (denoted as $\mathcal{H}_{V,\mu}^o$). Then,

$$\mathcal{H}_Q = \bigoplus_{V:|V|\leq Q} \mathcal{H}_V \tag{10}$$

$$= \bigoplus_{V:|V|\leq Q} \mathcal{H}_{V,\mu_\otimes}^o \tag{11}$$

$$= \bigoplus_{V:|V|\leq Q} \mathcal{H}_{V,\mu}^o. \tag{12}$$

If these equalities indeed hold, then we can use Theorem 3.9 to estimate f^* in $O(pQN^2 + N^3)$ time. Hence, it suffices to show how to take this estimate of f^* and compute its functional ANOVA decomposition with respect to μ instead of μ_\otimes (i.e., move from the parameterization in Eq. (11) to the one in Eq. (12)). We show how to compute this change-of-basis when all the $\mathcal{H}_{\{i\}}$ are finite-dimensional.

Assumption 4.3. For all $i \in [p]$ there exists a $B_i < \infty$ and linearly independent set of continuous functions $\{\phi_{ib}\}_{b=1}^{B_i}$ such that $\mathcal{H}_{\{i\}} = \text{span}\{1, \phi_{i1}, \dots, \phi_{iB_i}\}$ and $\Phi_i = [\phi_{i1}, \dots, \phi_{iB_i}]^T$.

Assumption 4.3 is a mild condition since we can approximate any function arbitrarily well by setting B_i sufficiently large given that $\mathcal{H}_{\{i\}}$ is separable; see Huang [1998] for rates of convergence for different finite-basis approximations. Under this assumption, Lemma 4.4 implies that $\mathcal{H}_{V,\mu_\otimes}^o = \mathcal{H}_{V,\mu}^o$. Hence, a change-of-basis formula exists. We provide the change-of-basis formula for $Q = 2$ in Theorem 4.5.

Lemma 4.4. *Under Assumption 3.12 and Assumption 4.3, any $f \in \mathcal{H}$ is square-integrable with respect to any probability measure.*

Theorem 4.5. *Suppose $Q = 2$ and that Assumption 3.12 and Assumption 4.3 hold. For $f \in \mathcal{H}$, let*

$$\begin{aligned} f &= f_\emptyset^{\mu_\otimes} + \sum_{i=1}^p f_{\{i\}}^{\mu_\otimes} + \sum_{i,j=1}^p f_{\{i,j\}}^{\mu_\otimes} \\ &= f_\emptyset^\mu + \sum_{i=1}^p f_{\{i\}}^\mu + \sum_{i,j=1}^p f_{\{i,j\}}^\mu \end{aligned}$$

be the functional ANOVA decompositions of f with respect to μ_\otimes and μ , respectively. Then, there exist unique coefficients, $\Psi_{ij}^i \in \mathbb{R}^{1 \times B_i}$, $\Psi_{ij}^j \in \mathbb{R}^{1 \times B_j}$, $\Psi_{ij}^0 \in \mathbb{R}$, such that

$$\begin{aligned} f_{\{i,j\}}^\mu(x_i, x_j) &= f_{\{i,j\}}^{\mu_\otimes}(x_i, x_j) - [\Psi_{ij}^i \Phi_i(x_i) + \Psi_{ij}^j \Phi_j(x_j) + \Psi_{ij}^0] \\ f_{\{i\}}^\mu(x_i) &= f_{\{i\}}^{\mu_\otimes}(x_i) + \sum_{p \geq j > i} \Psi_{ij}^i \Phi_i(x_i) + \sum_{1 \leq j < i} \Psi_{ji}^i \Phi_i(x_i) \\ f_\emptyset^\mu &= f_\emptyset^{\mu_\otimes} + \sum_{1 \leq i < j \leq p} \Psi_{ij}^0, \end{aligned} \tag{13}$$

where Φ_i denotes the (finite-dimensional) feature map in Definition 3.3.

We prove Theorem 4.5 in Appendix A.9. By Corollary 3.10, we can estimate $f_{\{i\}}^{\mu_\otimes}(x_i)$ and $f_{\{i,j\}}^{\mu_\otimes}(x_i, x_j)$ in time linear in p . Hence, it remains to show how we can actually compute each Ψ_{ij}^i in Theorem 4.5. In Section 5, we show how to estimate Ψ_{ij}^i arbitrarily well using a Monte Carlo approach.

5 Final algorithm and implementation details

We start by describing and motivating our choice of sparsity prior on κ . Then, we show how we fit κ and η using cross-validation and our computational tools in Section 3. We conclude by showing how we compute Ψ_{ij}^i in Theorem 4.5 via Monte Carlo.

Our Sparsity Inducing Prior on κ . To induce sparsity in κ for variable selection, we pick a prior on κ_i that equals the mixture of a discrete point mass at 0 and a $\text{Uniform}(0, 1)$ random variable. Similar to a *spike-and-slab* prior [George and McCulloch, 1993], the point mass at 0 allows us to achieve exact sparsity. Unlike a spike-and-slab prior, however, we construct our prior so that we can still take gradients (and hence use continuous optimization techniques like gradient descent); see Algorithm 1 for details. Our construction involves introducing another random variable U_i so that

$$\kappa_i = \frac{1}{1-c} \max(U_i - c, 0), \quad U_i \sim \text{Uniform}(0, 1). \quad (14)$$

Then, $\mathbb{P}(\kappa_i = 0) = c$. Otherwise, with probability $1 - c$, $\kappa_i \sim \text{Uniform}(0, 1)$. Hence, c plays a similar role as a prior inclusion probability in a spike-and-slab prior. Since κ_i is a deterministic function of U_i , it suffices to estimate U_i instead as we detail below.

Cross-Validation Loss and Optimization. Given the empirical success of cross-validation and its use in other functional ANOVA methods (e.g., as in Gu and Wahba [1993], Lin and Zhang [2006]), we also use cross-validation to fit the SKIM-FA kernel hyperparameters κ and η . Specifically, we would like to pick $U, \eta, \sigma_{\text{noise}}^2$ (where $\kappa_i = \frac{1}{1-c} \max(U_i - c, 0)$) by minimizing a leave- M -out cross validation loss:

$$\begin{aligned} L(U, \eta, \sigma_{\text{noise}}^2) &= \frac{1}{\binom{N}{M}} \sum_{\substack{A: A \subset [N] \\ |A|=N-M}} \left[\frac{1}{M} \sum_{m \in A} (y^{(m)} - \bar{f}_A(x^{(m)}))^2 \right], \\ &= \mathbb{E}_{A \sim \pi} \left[\frac{1}{M} \sum_{m \in A} (y^{(m)} - \bar{f}_A(x^{(m)}))^2 \right] \end{aligned} \quad (15)$$

where \bar{f}_A equals the kernel ridge regression fit in Eq. (6) using the subset of datapoints in A and

π equals the uniform distribution over all $N - M$ sized subsets A of $[N]$.

Since the gradient of $L(U, \eta, \sigma_{\text{noise}}^2)$ exists², we can minimize Eq. (15) using gradient descent. However, this loss is computationally intensive; we need to solve Eq. (6) $\binom{N}{M}$ times in order to take a single gradient descent step. Instead, we approximate Eq. (15) by using stochastic gradient descent. Specifically, we randomly draw a single A from π in Eq. (15) and use the mean-squared prediction error of \bar{f}_A to estimate Eq. (15). Then, this estimate leads to an unbiased estimate of Eq. (15), and hence the gradient of $L(U, \eta, \sigma_{\text{noise}}^2)$. We summarize our full procedure in Algorithm 1. Note that in Algorithm 1 we do not minimize over U but instead over \tilde{U} , where $U_i = \frac{\tilde{U}_i^2}{\tilde{U}_i^2 + 1}$. Since the range of $\frac{\tilde{U}_i^2}{\tilde{U}_i^2 + 1}$ equals $(0, 1)$ when \tilde{U}_i varies over all of \mathbb{R} , we can optimize \tilde{U}_i over an unconstrained domain.³

Proposition 5.1. *Suppose $\kappa_i^{(t)} = 0$ at some iteration t in Algorithm 1. Then, for all subsequent iterations $t' \geq t$, $\kappa_i^{(t')} = 0$.*

Based on Proposition 5.1, we may view Algorithm 1 as a gradient-based analogue of backward stepwise regression; we start with the full saturated model by initializing all $\tilde{U}_i = 1$ (and consequently all $\kappa_i > 0$). Then, we keep pruning off covariates the longer we run gradient descent. We demonstrate empirically in Section 7 that the actual data-generating covariates remain while the irrelevant covariates get pruned off. Once we have found the kernel hyperparameters from Algorithm 1, Algorithm 2 and Algorithm 3 show how to perform variable selection and recover the effects, respectively. Both Algorithm 2 and Algorithm 3 follow directly from Corollary 3.6 and Lemma 3.5.

Estimating Ψ_{ij}^i for Change-of-Basis Formula in Theorem 4.5. To estimate Ψ_{ij}^i , we use a Monte Carlo procedure in Algorithm 4.

Proposition 5.2. *Let $W \rightarrow \infty$ in Algorithm 4. Then, the components returned from Algorithm 4 converge to the decomposition in Eq. (13).*

²Although $\frac{1}{1-c} \max(U_i - c, 0)$ is not differentiable at c , we may instead take the sub-gradient. To compute gradients, we use the automatic differentiation library in `PyTorch`.

³Since we only care about estimating the κ_i , it does not matter that U_i is not a 1-1 function of \tilde{U}_i

Algorithm 1 Learn SKIM-FA Kernel Hyperparameters and Kernel Ridge Weights

```
1: procedure LEARNHYPERPARAMS( $M, \gamma, T$ )
2:   For all  $i \in [p]$ , set  $\tilde{U}_i^{(0)} = 1$ 
3:    $\eta^{(0)} = [1, \dots, 1]^T \in \mathbb{R}^Q$ 
4:    $\sigma_{\text{noise}}^{(0)} = \sqrt{0.5\text{var}(Y)}$   $\triangleright$  Initialize noise variance as half of the response variance
5:    $\tau^{(0)} = (\tilde{U}^{(0)}, \eta^{(0)}, \sigma_{\text{noise}}^{(0)})$ 
6:   for  $t \in 1 : T$  do  $\triangleright$  Update parameters via gradient descent
7:     Randomly select  $N - M$  datapoints and collect covariates and responses in  $X_A, Y_A$ 
8:     for  $i \in 1 : p$  do
9:        $U_i^{(t)} = \frac{[\tilde{U}_i^{(t)}]^2}{[\tilde{U}_i^{(t)}]^2 + 1}$ 
10:       $\kappa_i^{(t)} = \max(U_i^{(t)} - c, 0)$ 
11:    end for
12:    Compute kernel matrix  $K_\tau^A$ , where  $[K_\tau^A]_{ij} = k_{\text{SKIM-FA}}(X_i^A, X_j^A)$  via Eq. (8)
13:    Let  $f_A$  equal the solution of Eq. (6) with  $\lambda = [\sigma_{\text{noise}}^{(t)}]^2$ ,  $K = K_\tau^A$ ,  $Y = Y_A$ 
14:     $L = \frac{1}{M} \sum_{n \in [N] \setminus A} (y^{(n)} - f_A(x^{(n)}))^2$ 
15:     $\tau^{(t)} = \tau^{(t-1)} - \gamma \nabla_{\tau^{(t-1)}} L$   $\triangleright$  Compute gradients with automatic differentiation
16:  end for
17:  Compute  $\alpha^{(T)}$ , the kernel ridge regression weights found by solving Eq. (6) using all  $N$ 
    datapoints with SKIM-FA hyperparameters equal to  $\kappa^{(T)}, \eta^{(T)}, \sigma_{\text{noise}}^{(T)}$ 
18:  return  $\kappa^{(T)}, \eta^{(T)}, \sigma_{\text{noise}}^{(T)}, \alpha^{(T)}$ 
19: end procedure
```

Algorithm 2 SKIM-FA Variable Selection

```
1: procedure VARSELECT( $\kappa$ )
2:   return  $\{i : \kappa_i \neq 0\}$ 
3: end procedure
```

Algorithm 3 Estimated functional ANOVA effect \bar{f}_V of \bar{f}_θ with respect to μ_\otimes

```

1: procedure ORTHEFFECTS( $V, \alpha, \kappa, \eta, \alpha$ )
2:    $\theta_V = \eta_{|V|}^2 \prod_{i \in V} \kappa_i^2$ 
3:   return  $\bar{f}_V(\cdot) = \theta_V \sum_{n=1}^N \alpha_n k_V(x^{(n)}, \cdot)$ 
4: end procedure

```

Algorithm 4 Change of Basis Formula for Finite Dimensional Model Selection Kernels

```

1: procedure REEXPRESSEFFECT( $\alpha, k_\theta, W, \mu$ )
2:   Compute  $f_{\{i,j\}}^{\mu_\otimes}, f_{\{i\}}^{\mu_\otimes}, f_\emptyset^{\mu_\otimes}$  using Algorithm 3
3:   For  $1 \leq w \leq W$  randomly sample  $x^{(w)} \stackrel{\text{iid}}{\sim} \mu$ 
4:   Compute  $X_{ij} = [\Phi_i(x_i^{(1)}) \cdots \Phi_i(x_i^{(W)}) \Phi_j(x_j^{(1)}) \cdots \Phi_j(x_j^{(W)})]^T$ 
5:   Compute  $f_{ij,W}^{\mu_\otimes} = [f_{\{i,j\}}^{\mu_\otimes}(x_i^{(1)}, x_j^{(1)}) \cdots f_{\{i,j\}}^{\mu_\otimes}(x_i^{(W)}, x_j^{(W)})]^T$ 
6:   Compute  $[\hat{\Psi}_{ij}^i \hat{\Psi}_{ij}^j]^T = (X_{ij}^T X_{ij})^{-1} X_{ij}^T f_{ij,W}^{\mu_\otimes}$  ▷ Least-squares projection
7:   Compute  $\hat{f}_{\{i,j\}}^\mu = f_{\{i,j\}}^{\mu_\otimes} - [\hat{\Psi}_{ij}^i \Phi_i^T(\cdot) + \hat{\Psi}_{ij}^j \Phi_j^T(\cdot) + \Psi_{ij}^0]$ 
8:   Compute  $\hat{f}_{\{i\}}^\mu = f_{\{i\}}^{\mu_\otimes} + \sum_{j>i} \hat{\Psi}_{ij}^i \Phi_i(\cdot) + \sum_{j<i} \hat{\Psi}_{ji}^i \Phi_i(\cdot)$ 
9:   Compute  $\hat{f}_\emptyset^\mu = f_\emptyset^{\mu_\otimes} + \sum_{i<j} \hat{\Psi}_{ij}^0$ 
10:  return  $\hat{f}_{\{i,j\}}^\mu, \hat{f}_{\{i\}}^\mu, \hat{f}_\emptyset^\mu$ 
11: end procedure

```

6 Related Work

The foundational work by Gu and Wahba [1993] used a type of model selection kernel to estimate the functional ANOVA decomposition of f^* with splines. Since the method in Gu and Wahba [1993] does not lead to sparsity, Gunn and Kandola [2004], Lin and Zhang [2006] put an L_1 penalty on θ to achieve sparsity, similar to *multiple kernel learning* techniques [Lanckriet et al., 2004]. Adding an L_1 penalty does not lead to an analytical solution nor a convex optimization problem. Hence, Gunn and Kandola [2004], Lin and Zhang [2006] alternate between minimizing θ and recomputing \bar{f}_θ , similar to Algorithm 1. Other approaches use cross-validation and gradient descent to iteratively select θ [Gu and Wahba, 1993]. In either case, the computational bottleneck is computing and inverting $(K_\theta + \sigma_{\text{noise}}^2 I_{N \times N})^{-1} Y$: k_θ takes $O(p^Q)$ time to compute on a pair of

points. Hence, computing and inverting $K_\theta + \sigma_{\text{noise}}^2 I_{N \times N}$ take $O(p^Q N^2)$ time and $O(N^3)$ time, respectively.

Many existing functional ANOVA techniques assume that all covariates are independent, i.e., that μ equals the *product measure*; see, for example, Gunn and Kandola [2004], Lin and Zhang [2006], Gu and Wahba [1993], Durrande et al. [2013]. Hooker [2007] highlighted pathologies that arise when using μ_\otimes instead of μ . Specifically, he empirically showed on synthetic and real data that the functional ANOVA decomposition of an $f \in \mathcal{H}$ with respect to μ can be significantly different than the decomposition with respect to μ_\otimes . This discrepancy arises because μ_\otimes can place high probability in regions where the actual covariate distribution μ has low probability; see also Section 4.1.

7 Experiments

Summary of Experimental Results. In this section, we compare our inference methods in Section 5 against existing procedures in terms of variable selection and estimation performance. We find that when the interaction effects are strong or comparable to the strength of the additive effects, our method outperforms existing methods in terms of variable selection and estimation performance. When the interaction effects are weak our method does not (uniformly) have the best performance but still performs well relative to many of the other methods.⁴

There are two immediate challenges with our empirical evaluation. The first is that existing methods estimate the functional ANOVA decomposition assuming all covariates are independent (or sometimes do not even specify the measure). Hence, we start our evaluation by assuming the covariates are independent so that we can compare against existing methods in Section 7.3 and Section 7.4. Then, in Section 7.5, we show why the assumption of independent covariates is problematic to demonstrate the practical utility of Algorithm 4.

The second challenge concerns our performance metrics (detailed in Section 7.1 and Section 7.2), which require knowing the ground truth effects. Since we do not know the ground truth effects in real data, we start in Section 7.3 by evaluating each method on simulated data so that we have

⁴All results can be re-generated using the data and code provided in <https://github.com/agrawalraj/skimfapaper>

ground truth effects. To compare methods on real data, we use a similar evaluation procedure as in Agrawal et al. [2019] to construct a synthetic ground truth for benchmarking (see Section 7.4 for details).

7.1 Benchmark Methods

We compare our method against other methods used to model high-dimensional data and interactions. We focus on the $Q = 2$ case throughout since (1) existing methods typically only work for the pairwise interaction case and (2) higher-order interactions are often difficult to interpret and estimate. Even when $Q = 2$, the functional ANOVA methods outlined in Section 7.1 take $O(p^2 N^2 + N^3)$ time, making them computationally intractable for even moderate p and N settings. Instead, we focus on methods that can model interactions and actually scale to moderate-to-large p and N settings. These methods include approximate “two-stage” and greedy forward-stage regression methods, and linear interaction models. We detail these approaches in more depth in Appendix B. The list below summarizes the candidate methods (and software implementations) that we select from each category for empirical evaluation.⁵

- **SPAM-2Stage**: we perform variable selection by fitting a sparse additive model (SpAM) [Liu et al., 2008] to the data. We use the `sam` package in R. Since `sam` does not provide a default way to select the L_1 regularization strength, we use 5-fold cross-validation. For estimation, we generate all main and interaction effects among the subset of covariates selected by SpAM. We calculate these effects by taking pairwise products of univariate basis functions generated from a cubic spline basis with 5 total knots; see Appendix C for details. We estimate the basis coefficients (and hence effects) using ridge regression, where again we use 5-fold cross-validation to pick the L_2 regularization strength.

- **Multivariate Additive Regression Splines (MARS)**: we use the `python` implemen-

⁵Agrawal et al. [2019] fit linear interaction models in $O(pN^2 + N^3)$ time per iteration, which has the same asymptotic complexity as Algorithm 1. However, they use Hamiltonian Monte Carlo (HMC) to perform inference. Each HMC step requires computing and inverting an $N \times N$ kernel matrix many times. Hence, their method takes hours to complete when p and N are larger than 500. Due to this computational intensity, we do not benchmark against their method.

tation of MARS [Friedman, 1991] in `py-earth`. We consider two functional ANOVA decompositions of the fitted regression function:

- **MARS-Vanilla**: the main effect of each covariate equals the sum of all selected univariate basis functions of that covariate (i.e., after the pruning step of MARS). Similarly, each pairwise effect equals the sum of all selected bivariate basis functions of those two covariates. This is the functional ANOVA decomposition originally proposed in Friedman [1991] and the one actually implemented in existing MARS software packages. It is unclear, however, what measure this functional ANOVA decomposition is taken with respect to.
- **MARS-EMP**: to the best of our knowledge, there currently does not exist a procedure to perform the functional ANOVA decomposition of MARS with respect to the empirical distribution of the covariates. We describe how to perform such a decomposition when the covariates are jointly independent in Appendix E, which could be of independent interest.
- **Hierarchical Lasso (HierLasso)**: we use the implementation of HierLasso [Lim and Hastie, 2015] in the authors’ R package `glinternet`. Since Lim and Hastie [2015] use cross-validation to pick the L_1 regularization strength, we similarly use 5-fold cross-validation.
- **Pairs Lasso**: we fit the Lasso on the expanded set of features $\{x_i\}_{i=1}^p$ and $\{x_i x_j\}_{i,j=1}^p$. We fit the Lasso using the python package `sklearn`, and use 5-fold cross-validation to select the L_1 regularization strength.

7.2 Evaluation Metrics

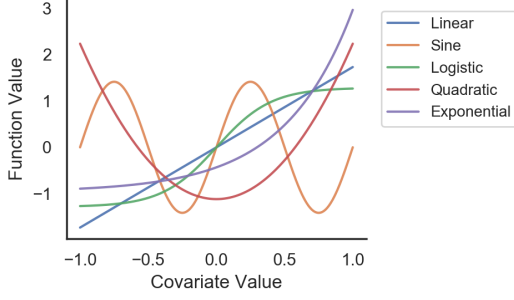
Variable Selection Evaluation Metrics. We consider both the power to select correct covariates and avoid incorrect ones.

- **# Correct Selected**: we count the number of covariates correctly selected by the method. Higher is better.

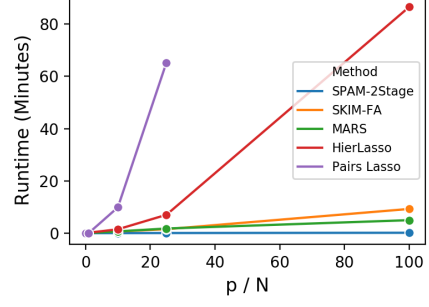
- # Wrong Selected: we count the number of covariates incorrectly selected by the method (i.e., Type I error). Lower is better.
- # Correct Not Selected: we count the number of covariates that belong to the true model but were not selected by the method (i.e., Type II error). Lower is better.

Estimation Evaluation Metrics. We evaluate how well a method estimates main effects and interaction effects. Instead of looking only at the total mean squared estimation error, we break this error into multiple buckets to understand what bucket drives the majority of the error. Lower is better for all of the quantities below.

- Correct Selected SSE (Main): we take the sum of squared errors (SSE) between each estimated main effect component and true main effect component. This sum equals $\sum_{i \in S_1} \|f_i^* - \hat{f}_i\|_\mu^2$, where S_1 is the set of correctly identified main effects, \hat{f}_i is the estimated main effect, and f_i^* is the true main effect.
- Correct Not Selected SSE (Main): we take the sum of squared norms of main effects not selected. This sum equals $\sum_{i \in S_2} \|f_i^*\|_\mu^2$, where S_2 is the set of correct main effects not selected.
- Wrong Selected SSE (Main): we take the sum of squared norms of main effect components incorrectly selected. This sum equals $\sum_{i \in S_3} \|\hat{f}_i\|_\mu^2$, where S_3 is the set of incorrect main effects selected.
- Correct Selected SSE (Pair): this metric is the same as Correct Selected SSE (Main) except that it counts the number of correctly selected interactions
- Correct Not Selected SSE (Pair): this metric is the same as Correct Not Selected SSE (Main) except that it counts the number of correct interactions not selected
- Wrong Selected SSE (Pair): this metric is the same as Wrong Selected SSE (Main) except that it counts the number of interactions incorrectly selected
- Total SSE: this metric equals the sum of the 6 buckets above



(a) Synthetic Data Test Functions



(b) Runtimes on Simulated Data

Figure 2: The left hand plot provides the test functions used to generate synthetic data. The left hand plot compares the runtime of different methods as p/N increases.

- **Total SSE / Signal Variance:** this metric equals the relative estimation error, i.e., Total SSE divided by the true signal variance.

7.3 Synthetic Data Evaluation

We randomly generate covariates and responses as follows. For the covariates, we draw each data point and covariate dimension $x_i^{(n)} \stackrel{\text{iid}}{\sim} \text{Uniform}([-1, 1])$. Since $[-1, 1]$ is compact, Theorem 2.1 ensures that the functional ANOVA decomposition is unique. We let y depend on the first 5 covariates; the remaining $p - 5$ covariates are taken as noise covariates that we do not want to select. To generate responses reflective of what we might expect in real data, we consider the 5 trends shown in Fig. 2a: linear, sine, logistic, quadratic, and exponential. We let the main effects equal the sum of these 5 trends, where the i th trend is applied to covariate i . For the interactions between the first 5 covariates, we consider all pairwise products of the 5 trends above, resulting in 10 total interactions. We select a noise variance such that the $R^2 = \frac{\sigma_{\text{signal}}^2}{\sigma_{\text{signal}}^2 + \sigma_{\text{noise}}^2} = 0.8$, where $\sigma_{\text{signal}}^2 = \langle f^*, f^* \rangle_\mu$. We further decompose the signal variance in terms of the total variance explained by main effects and interactions. Similar to the empirical evaluations in Lim and Hastie [2015], we consider the following three settings:

- **Main Effects Only:** each of the 5 main effects has 1/5th of the total signal variance, and

Table 1: Synthetic Data Variable Selection Performance Results for $p = 1000$. The method with the fewest number of incorrect covariates selected is bolded.

Method	Setting	# Correct Selected	# Wrong Selected	# Correct Not Selected
SKIM-FA	Main-Only	3	0	2
MARS	Main-Only	5	70	0
SPAM-2Stage	Main-Only	5	15	0
HierLasso	Main-Only	4	5	1
Pairs Lasso	Main-Only	4	6	1
SKIM-FA	Equal	5	0	0
MARS	Equal	4	71	0
SPAM-2Stage	Equal	5	15	0
HierLasso	Equal	4	40	0
Pairs Lasso	Equal	5	213	0
SKIM-FA	Weak Main	5	9	0
MARS	Weak Main	5	75	0
SPAM-2Stage	Weak Main	1	41	4
HierLasso	Weak Main	5	120	0
Pairs Lasso	Weak Main	5	144	0

each pairwise effect has 0 signal variance (i.e., no pairwise interactions).

- **Equal Main and Interaction Effects:** each main effect and pairwise effect has $0.5 * 1/5$ and $0.5 * (1 / 10)$ of the total signal variance, respectively. Hence, the total main effect variance equals the total pairwise signal variance.
- **Weak Main Effects:** each main effect and pairwise effect has $0.01 * 1/5$ and $0.99 * (1 / 10)$ of the total signal variance, respectively. Hence, the total main effect and pairwise effect variances equal 1% and 99% of the total signal variance, respectively.

To test the impact of increasing dimensionality on inference quality, we consider $p \in \{250, 500, 1000\}$ and keep $N = 1000$ fixed for each setting.

We summarize the variable selection and estimation performances of each method for $p = 1000$

Table 2: Synthetic Data Estimation Performance Results for $p = 1000$. The method with the smallest total SSE is bolded.

Method	Setting	Correct Selected SSE (Main)	Correct Not Selected SSE (Main)	Wrong Selected SSE (Main)	Correct Selected SSE (Pair)	Correct Not Selected SSE (Pair)	Wrong Selected SSE (Pair)	Total SSE	÷ Signal Variance
SKIM-FA	Main Only	2.7	8.1	0	0	0	0.24	11.03	0.55
SPAM-2Stage	Main Only	2.67	0	0.78	0	0	0.02	3.46	0.17
MARS-EMP	Main Only	0.45	0	2.68	0	0	2.39	5.51	0.28
MARS-VANILLA	Main Only	16.14	0	1.56	0	0	10.33	28.02	1.4
SKIM-FA	Equal	1.54	0	0	0.29	0	0	1.82	0.09
SPAM-2Stage	Equal	1.67	0	1.07	0.41	0	2.16	5.31	0.27
MARS-EMP	Equal	0.61	0	3.84	1.7	0	2.52	8.67	0.43
MARS-VANILLA	Equal	454.88	0	3.16	21.46	0	13.22	492.72	24.64
SKIM-FA	Weak Main	0.72	0	1.37	0.61	0	0.63	3.33	0.17
SPAM-2Stage	Weak Main	0.16	0.2	6.69	0	18.33	0.31	25.69	1.28
MARS-EMP	Weak Main	0.67	0	5.86	3.37	0	5.63	15.52	0.78
MARS-VANILLA	Weak Main	23.62	0	3.18	23.16	0	15.43	65.39	3.27

in Table 1 and Table 2, respectively; see Appendix F for model performance results for all choices of p . As we discuss below, SKIM-FA outperforms all of the other methods (in terms of both variable selection and estimation) in the Weak Main Effects and the Equal Main and Interaction settings. For the Main Effects Only setting, SKIM-FA selects the fewest number of incorrect covariates. Since SKIM-FA does not select two of the correct covariates in this setting, however, its estimation performance is worse than some of the other benchmark methods.

Weak Main Effects Setting. In the setting of weak main effects, both Spam-2Stage and MARS perform much worse than the other methods. Spam-2Stage selects only one correct covariate for $p = 500$ and $p = 1000$. This poor variable selection is expected since the signal is locked away in the interactions but SpAM assumes additive effects. In particular, only 1% of the variance is explained by additive effects (even though additive *and* interaction effects explain 80% of the variance in the response). Since Spam-2Stage only considers interactions between covariates

selected by SpAM, its poor estimation performance is driven by not selecting many of the correct covariates.

Similar to Spam2Stage, MARS performs poorly because it can only form an interaction between two covariates if at least one of the covariates has an additive effect. In the extreme case of no additive effects, for example, MARS randomly selects covariates to have additive effects. By random chance, MARS will eventually select a correct covariate (i.e., one the response actually depends on) to have an additive effect. Since this covariate has an interaction effect, in the next step MARS will (likely) select the correct interaction effect. Hence, MARS will need to select many incorrect covariates as additive effects before identifying the true interactions.

For estimation, we compare only the nonlinear methods; linear methods will artificially perform poorly since some of the effects are highly nonlinear by construction. Evaluating estimation performance is trickier than evaluating selection performance since the functional ANOVA decomposition depends on the choice of measure. Unless otherwise stated, the target of inference is finding the functional ANOVA decomposition of f^* with respect to μ (the joint distribution of the covariates).

Since MARS-VANILLA performs a functional ANOVA decomposition with respect to an unspecified measure, it is unclear how to interpret its main and interaction effects. One might think (and truthfully what we initially thought) that MARS-VANILLA would still return a functional decomposition close to one with respect to the actual covariate distribution. Table F.6 shows that this intuition is incorrect; the relative estimation error of MARS-VANILLA always exceeds 1! This poor estimation performance stems from not specifying the measure (and hence the target of inference), not MARS’s ability in finding a model with good predictive performance. In particular, MARS-EMP, which produces the *exact same predictions* as MARS-VANILLA, yields much better estimation performance because it re-orthogonalizes the fit with respect to the actual covariate distribution.

Equal Main and Interaction Effects Setting. We summarize the variable selection and estimation performances of each method in Table F.3 and Table F.4, respectively. In this setting, all methods are able to recover all 5 true covariates. For both estimation and variable selection,

SKIM-FA performs better than the other methods.

Main Effects Only Setting. We summarize the variable selection and estimation performances of each method for $p = 1000$ in Table 1 and Table 2, respectively. Appendix F contains the results for the remaining choices of p ; see Table F.1 and Table F.2. Each method selects the majority of correct covariates. However, some methods – namely Pairs Lasso and HierLasso – have a systematic bias; for all choices of p , they never select covariate 3 (the quadratic trend) since a quadratic trend has a weak linear correlation. Since the other methods can model nonlinear relationships, they can pick up this trend. Hence, they have better statistical power to detect correct covariates, improving variable selection performance.

In terms of Type I error, some methods select incorrect covariates much more frequently than others. For example, MARS consistently selects over 50 incorrect covariates for all choices of p . A potential explanation of this poor performance is that MARS induces sparsity through a greedy pruning step instead of an actual sparsity inducing penalty as in the other methods.

Runtime Comparisons. We conclude this section by comparing each method in term of runtime. The two Lasso methods which take $O(p^2N)$ time, but the remaining methods depend only linearly on p . When $p > N$, our method takes $O(\kappa N^3)$ while the two Lasso based methods take $O(\kappa^2 N^3)$ time, where $\kappa = p/N$. Hence, for higher-dimensional problems, our method will become much faster relative to the Lasso methods. For example, in genome-wide association studies, datasets can have N on the order of 10^3 and p on the order of 10^7 [1000 Genomes Project, 2015]. Hence, $\kappa = 10^4$, which corresponds to a potential 10^4 computational speedup factor. In Fig. 2b, we compare the runtimes of each method as we vary p/N on simulated data. We keep N fixed at 100 and vary p from 10 to 10^4 . As expected, as p/N increases, our method yields substantial computational savings relative to Pairs Lasso and HierLasso. Relative to Spam-2Stage and MARS, our method does not yield better computational scaling. However, based on our synthetic evaluation above (and real data evaluation in Section 7.4), we have better statistical performance.

Table 3: Variable Selection Performance for the Bike Sharing Dataset.

Method	# Covariates	# Original Selected	# Wrong Selected
SKIM-FA	1000	3	0
HierLasso	1000	3	5
SPAM-2Stage	1000	3	8
Pairs Lasso	1000	3	76
MARS	1000	3	119

7.4 Evaluation on Real Data

Evaluating the methods in terms of variable selection and estimation quality is challenging because we typically do not have ground truth main and interaction effects for high-dimensional (real) data. Similar to the evaluation procedure in Agrawal et al. [2019], we instead take a low-dimensional dataset where N is large and p is small. We make it high-dimensional by adding synthetic random noise covariates. These two choices have several purposes. First, by fitting a regression function on the original low-dimensional dataset, standard $N^{-1/2}$ statistical convergence rates apply. Hence, for large N , a maximum-likelihood estimate of the regression function will be close to the true regression function, creating a (near) ground truth for estimation evaluation. For variable selection, the random noise covariates create a “synthetic control;” if a method selects any of the random noise covariates as a main or interaction effect, we know the method selected an incorrect covariate.

Based on these ideas, we consider the popular (low-dimensional) Bike Sharing dataset, which we downloaded from the UCI Machine Learning Repository. This dataset contains 17,389 datapoints and 13 covariates. We consider 4 continuous variables (hour, air temperature, humidity, windspeed) and use the total number of bikes rented as the response. We standardize the response by subtracting the mean and dividing by the standard deviation, and min-max standardize the covariates so that each covariate belongs to $[0, 1]$. For the proxy ground truth, we fit a pairwise interaction model consisting of all 4 main effects and 6 possible pairwise interactions.

Similar to our synthetic evaluation, we randomly subsample a total of $N = 10^3$ datapoints,

Table 4: Estimation Performance for the Bike Sharing Dataset.

Method	# Noise	Correct Selected SSE (Main)	Correct Not Selected SSE (Main)	Wrong Selected SSE (Main)	Correct Selected SSE (Pair)	Correct Not Selected SSE (Pair)	Wrong Selected SSE (Pair)	Total SSE
SKIM-FA	1000	0.145	0.002	0	0.107	0.009	0	0.263
SPAM-2Stage	1000	0.149	0.002	0.027	0.081	0.009	0.000	0.269
MARS-EMP	1000	0.214	0.002	0.485	0.054	0.026	0.245	1.026
MARS-Vanilla	1000	6.556	0.002	0.796	0.947	0.026	1.882	10.209

and then train each benchmark method on this subsampled dataset. To make the inference task high-dimensional we inject $p_{\text{noise}} \in \{250, 500, 1000\}$ random noise covariates, where these noise covariates are drawn iid from a Uniform(0, 1) distribution. We report on the same variable selection and estimation metrics as in the synthetic experiments for $p_{\text{noise}} = 1000$ in Table 3 and Table 4, respectively; see Table F.8 and Table F.9 for all choices of p_{noise} . We see that again SKIM-FA has similar or much better estimation and variable selection performance relative to the other methods. Finally, to understand the impact of correlated predictors on performance, we append correlated (real) covariates to the Bike Sharing dataset (instead of synthetic ones drawn from a Uniform(0, 1) distribution) in Appendix F.1. We again find that SKIM-FA has better performance than the other methods.

7.5 Impact of Correlated Predictors on the Functional ANOVA

So far we have performed the functional ANOVA decomposition assuming that the covariates are jointly independent; for our synthetic data evaluation in Section 7.3 this independence held by design. Here we show the effect correlated predictors have on the resulting decomposition. Recall that previous functional ANOVA methods assume product measure, but our Algorithm 4 provides the flexibility to select different measures. We demonstrate the practical utility of this flexibility here. To this end, we consider the simplest possible regression function with

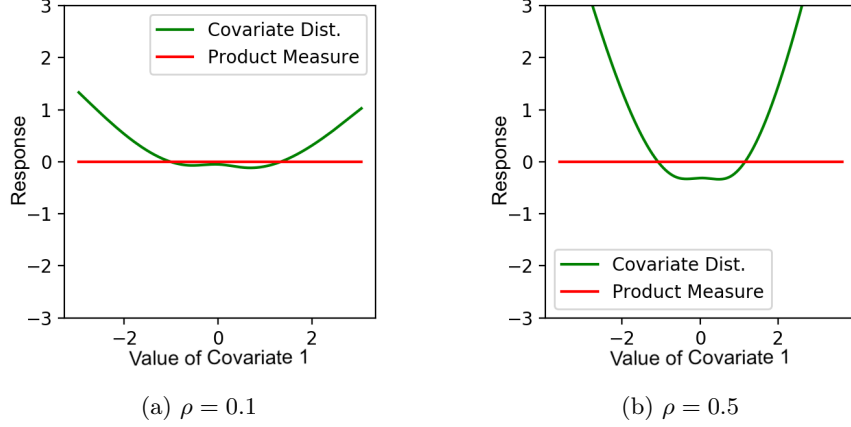
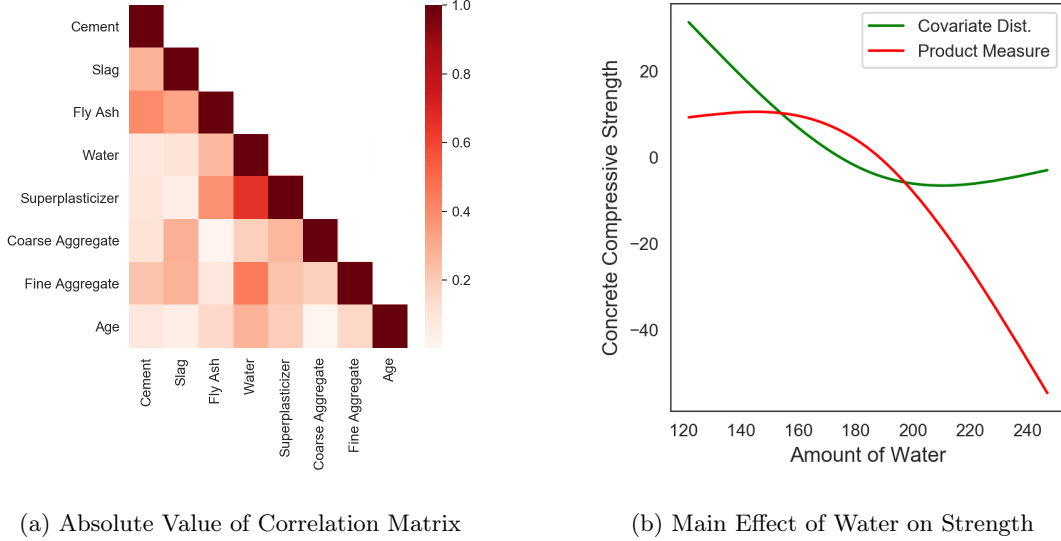


Figure 3: The left hand and right hand plots show how the additive effect of x_1 (in the functional ANOVA decomposition of the function x_1x_2) varies as the correlation between x_1 and x_2 increases.

interactions: $f(x_1, x_2) = x_1x_2$. If $x_1 \perp\!\!\!\perp x_2$, then the functional ANOVA decomposition of f with respect to $\mu(x_1, x_2)$ equals x_1x_2 . However, if x_1 and x_2 are correlated, then the functional ANOVA decomposition no longer equals x_1x_2 . In particular, as the correlation between x_1 and x_2 increases, f can be explained better by additive effects (e.g., in the degenerate case when $x_1 = x_2$, then $f(x_1, x_2) = x_1^2$). To test this empirically, we randomly generate x_1, x_2 from a multivariate Gaussian distribution with marginal variances equal to 1 and pairwise correlation equal to ρ . We let $\rho \in \{0.1, 0.5\}$. Fig. 3 shows that when ρ gets stronger, the discrepancy between a functional ANOVA decomposition with respect to $\mu(x_1, x_2)$ versus product measure $\mu_{\otimes} = N(0, 1) \otimes N(0, 1)$ increases. As expected, as the correlation increases, a quadratic-like function of x_1 and x_2 explains f increasingly well.

We perform a similar analysis above but for real data, namely the Concrete Compressive Strength dataset from the UCI machine learning repository.⁶ In Fig. 4, we plot the correlations between the 8 covariates that potentially predict the response (concrete strength). The two most correlated covariates are the amount of water and the amount of superplasticizer. Since

⁶In Appendix F.2, we compare how the functional ANOVA decomposition changes depending on if we use μ or μ_{\otimes} for the Bike Sharing dataset. Unlike the Concrete Compressive Strength dataset, however, we do not see a large difference between the two functional ANOVA decompositions for the Bike Sharing dataset.



(a) Absolute Value of Correlation Matrix

(b) Main Effect of Water on Strength

Figure 4: Effect of Correlated Predictors on the Concrete Compressive Strength Dataset

the covariates have non-trivial correlations, the functional ANOVA decomposition with respect to μ and μ_{\otimes} might be different based on Proposition 4.1. In Fig. 4 we see that there indeed is a difference; the (estimated) additive effect for water on concrete strength varies substantially depending on which measure is selected to perform the functional ANOVA decomposition.

8 Concluding Remarks

In this paper, we developed a new, computationally efficient method to perform sparse functional ANOVA decompositions. The heart of our procedure relied on a new kernel trick to implicitly represent nonlinear interactions (Theorem 3.9), and a change-of-basis formula (Theorem 4.5) to re-express the fit in terms of an arbitrary measure. We compared our method against other methods often used to model high-dimensional data with interactions. We found improved performance on both simulated and real datasets by relaxing assumptions such as linearity and the presence of strong-additive effects while still remaining competitive (or being orders of magnitude faster) in terms of runtime.

There are many interesting future research directions. One involves scaling our method to both the large N and p setting; our current method takes $O(pQN^2 + N^3)$ time which becomes problematic for large N . This cubic dependence, however, is not unique to our method but rather a fundamental obstacle faced by kernel ridge regression and Gaussian processes. Fortunately, many methods already exist to help alleviate these computational challenges with respect to N ; see, for example, Gardner et al. [2018], Titsias [2009], Quiñonero Candela and Rasmussen [2005]. Another interesting direction involves applying our method to real biological datasets. In particular, an open challenge in genomics has been detecting *epistasis*, or interaction effects between genetic variants, from genome sequencing data [Maher, 2008, Aschard, 2016, Slim et al., 2018, Greene et al., 2010]. Detecting epistasis has been statistically and computationally challenging because p is in the millions, so the number of pairwise interactions is on the order of *trillions*. Since our method does not require explicitly generating all interactions, it has the potential to tractably detect interactions in such especially high-dimensional data regimes.

References

- C. 1000 Genomes Project. A global reference for human genetic variation. *Nature*, 526:68–74, 2015.
- R. Agrawal, B. Trippe, J. Huggins, and T. Broderick. The kernel interaction trick: Fast Bayesian discovery of pairwise interactions in high dimensions. In *International Conference on Machine Learning*, 2019.
- H. Aschard. A perspective on interaction effects in genetic association studies. *Genetic Epidemiology*, 2016.
- J. Bien, J. Taylor, and R. Tibshirani. A Lasso for hierarchical interactions. *The Annals of Statistics*, 41(3):1111–1141, 2013.
- E. Candes and T. Tao. The Dantzig selector: Statistical estimation when p is much larger than n . *The Annals of Statistics*, pages 2313–2351, 2007.

- S. Chen, D. Donoho, and M. Saunders. Atomic decomposition by basis pursuit. *SIAM Journal on Scientific Computing*, pages 33–61, 1998.
- H. Chipman. Bayesian variable selection with related predictors. *The Canadian Journal of Statistics*, 24(1):17–36, 1996.
- S. M. Curtis, S. Banerjee, and S. Ghosal. Fast Bayesian model assessment for nonparametric additive regression, 2014.
- N. Durrande, D. Ginsbourger, O. Roustant, and L. Carraro. ANOVA kernels and RKHS of zero mean functions for model-based sensitivity analysis. *Journal of Multivariate Analysis*, 115(C): 57–67, 2013.
- F. Ferrari and D. B. Dunson. Bayesian factor analysis for inference on interactions. *Journal of the American Statistical Association*, 0(0), 2020a.
- F. Ferrari and D. B. Dunson. Identifying main effects and interactions among exposures using Gaussian processes. *The Annals of Applied Statistics*, 14(4), 2020b.
- J. H. Friedman. Multivariate adaptive regression splines. *Annals of Statistics*, 19(1):1–67, 1991.
- J. Gardner, G. Pleiss, K. Q. Weinberger, D. Bindel, and A. G. Wilson. GPyTorch: Blackbox matrix-matrix Gaussian process inference with GPU acceleration. In *Advances in Neural Information Processing Systems*, 2018.
- E. George and R. McCulloch. Variable selection via Gibbs sampling. *Journal of the American Statistical Association*, 88(423):881–889, 1993.
- C. Greene, N. Sinnott-Armstrong, D. S. Himmelstein, P. Park, J. Moore, and B. Harris. Multifactor dimensionality reduction for graphics processing units enables genome-wide testing of epistasis in sporadic ALS. *Bioinformatics*, 26(5):694–695, 2010.
- J. Griffin and P. Brown. Hierarchical shrinkage priors for regression models. *Bayesian Analysis*, 12:135–159, 2017.

- C. Gu and G. Wahba. Smoothing spline ANOVA with component-wise Bayesian “confidence intervals”. *Journal of Computational and Graphical Statistics*, 2(1):97–117, 1993.
- S. Gunn and J. Kandola. Structural modelling with sparse kernels. *Machine Learning*, 48:137–163, 2004.
- G. Hooker. Generalized functional anova diagnostics for high-dimensional functions of dependent variables. *Journal of Computational and Graphical Statistics*, 16(3):709–732, 2007.
- D. Hsu, S. M. Kakade, and T. Zhang. Random design analysis of ridge regression. *Foundations of Computational Mathematics*, 14(3):569–600, 2014.
- J. Z. Huang. Projection estimation in multiple regression with application to functional ANOVA models. *Annals of Statistics*, 26(1):242–272, 1998.
- G. R. G. Lanckriet, N. Cristianini, P. Bartlett, L. E. Ghaoui, and M. I. Jordan. Learning the kernel matrix with semidefinite programming. *Journal of Machine Learning Research*, page 27–72, 2004.
- M. Lim and T. Hastie. Learning interactions via hierarchical group-lasso regularization. *Journal of Computational and Graphical Statistics*, 24(3):627–654, 2015.
- Y. Lin and H. H. Zhang. Component selection and smoothing in multivariate nonparametric regression. *Annals of Statistics*, 34(5):2272–2297, 2006.
- H. Liu, L. Wasserman, J. D. Lafferty, and P. K. Ravikumar. Spam: Sparse additive models. 2008.
- Y. Lou, R. Caruana, J. Gehrke, and G. Hooker. Accurate intelligible models with pairwise interactions. In *International Conference on Knowledge Discovery and Data Mining*, 2013.
- B. Maher. Personal genomes: The case of the missing heritability. *Nature*, pages 18–21, 2008.
- C. A. Micchelli, Y. Xu, and H. Zhang. Universal kernels. *Journal of Machine Learning Research*, 7:2651–2667, 2006.

- K. Nakagawa, S. Suzumura, M. Karasuyama, K. Tsuda, and I. Takeuchi. Safe pattern pruning: An efficient approach for predictive pattern mining. In *International Conference on Knowledge Discovery and Data Mining*, 2016.
- J. Quiñonero Candela and C. E. Rasmussen. A unifying view of sparse approximate Gaussian process regression. *Journal of Machine Learning Research*, 6:1939–1959, 2005.
- C. E. Rasmussen and C. K. I. Williams. *Gaussian Processes for Machine Learning*. The MIT Press, 2006.
- S. Rendle. Factorization machines. pages 995–1000, 2010.
- F. Scheipl, L. Fahrmeir, and T. Kneib. Spike-and-slab priors for function selection in structured additive regression models. *Journal of the American Statistical Association*, 107(500):1518–1532, 2012.
- R. Shah. Modelling interactions in high-dimensional data with backtracking. *Journal of Machine Learning Research*, 17(207):1–31, 2016.
- L. Slim, C. Chatelain, C. Azencott, and J. Vert. Novel methods for epistasis detection in genome-wide association studies. *bioRxiv:325993*, 2018.
- C. J. Stone. The use of polynomial splines and their tensor products in multivariate function estimation. *Annals of Statistics*, 22(1):118–171, 1994.
- M. K. Titsias. Variational learning of inducing variables in sparse Gaussian processes. In *International Conference on Artificial Intelligence and Statistics*, pages 567–574, 2009.
- V. N. Vapnik. *The nature of statistical learning theory*. Springer-Verlag, 1995.
- R. Wei, B. Reich, J. Hoppin, and S. Ghosal. Sparse Bayesian additive nonparametric regression with application to health effects of pesticides mixtures. *Statistica Sinica*, 2019.

SUPPLEMENTARY MATERIAL

A Proofs

A.1 Proof of Proposition 3.2

It suffices to prove that \mathcal{H}_V^o is an RKHS. First we prove that \mathcal{H}_V^o is a Hilbert space. Since $\mathcal{H}_V^o \subset \mathcal{H}_V$, it suffices to show that \mathcal{H}_V^o is a vector space and complete. To show that \mathcal{H}_V^o is a vector space, take arbitrary $f, g \in \mathcal{H}_V^o$ and $\alpha, \beta \in \mathbb{R}$. We want to show $\alpha f + \beta g \in \mathcal{H}_V^o$. Take an arbitrary $f_A \in \mathcal{H}_A$, $A \subsetneq V$. Then,

$$\begin{aligned} \langle \alpha f + \beta g, f_A \rangle_\mu &= \alpha \langle f, f_A \rangle_\mu + \beta \langle g, f_A \rangle_\mu \\ &= 0 \end{aligned}$$

since $f, g \in \mathcal{H}_V^o$. Hence, \mathcal{H}_V^o is a vector space.

Suppose towards a contradiction that \mathcal{H}_V^o is not complete. Then, since \mathcal{H}_V is complete, there exists an $f' \in \mathcal{H}_V \setminus \mathcal{H}_V^o$ and Cauchy sequence $\{f_n\}_{n=1}^\infty$ such that $\lim_{n \rightarrow \infty} \|f' - f_n\|_{\mathcal{H}_V} = 0$, where $f_n \in \mathcal{H}_V^o$ and $\|\cdot\|_{\mathcal{H}_V}$ denotes the induced RKHS norm for \mathcal{H}_V . Then, there exists an $\epsilon > 0$ and $f_A \in \mathcal{H}_A$, $A \subsetneq V$ such that

$$\begin{aligned} \epsilon &= \langle f', f_A \rangle_\mu \\ &= \langle f' + f_m - f_m, f_A \rangle_\mu \\ &= \langle f' - f_m, f_A \rangle_\mu + \langle f_m, f_A \rangle_\mu \\ &= \langle f' - f_m, f_A \rangle_\mu \\ &\leq \|f' - f_m\|_\mu \|f_A\|_\mu \quad (\text{by Cauchy-Schwarz}). \end{aligned} \tag{16}$$

To reach a contradiction, it suffices to show that there exists an $m < \infty$ such that $\|f' - f_m\|_\mu < \frac{\epsilon}{\|f_A\|_\mu}$. To obtain this inequality, we upper bound $\|\cdot\|_\mu$ in terms of $\|\cdot\|_{\mathcal{H}_V}$. Let r_V be the reproducing kernel for \mathcal{H}_V . Then, for $f \in \mathcal{H}_V$,

$$\begin{aligned} |f(x)|^2 &= |\langle f, r_V(x, \cdot) \rangle_{\mathcal{H}_V}|^2 \quad (\text{by the reproducing property}) \\ &\leq \|f\|_{\mathcal{H}_V}^2 r_V(x, x)^2 \quad (\text{by Cauchy-Schwarz}). \end{aligned} \tag{17}$$

Then,

$$\begin{aligned}\|f\|_\mu^2 &= \int |f(x)|^2 d\mu \\ &\leq \|f\|_{\mathcal{H}_V}^2 \int r_V(x, x)^2 d\mu\end{aligned}\tag{18}$$

Since \mathcal{H}_V belongs to the space of square integrable functions, $\int r_V(x, x)^2 d\mu = M_V < \infty$. Hence,

$$\|f' - f_m\|_\mu \leq M_V \|f' - f_m\|_{\mathcal{H}_V}^2 < \infty.\tag{19}$$

Since $\|f' - f_m\|_{\mathcal{H}_V}^2 \rightarrow 0$, there exists an m such that $\|f' - f_m\|_\mu < \frac{\epsilon}{\|f_A\|_\mu}$. Hence, \mathcal{H}_V^o is complete.

To complete the proof it suffices to show that the evaluation functional on \mathcal{H}_V^o is a bounded operator. Since \mathcal{H}_V is an RKHS there exists an $M_x < \infty$ such that for all $f \in \mathcal{H}_V$

$$|f(x)| \leq M_x \|f\|_{\mathcal{H}_V}.\tag{20}$$

Since $\mathcal{H}_V^o \subset \mathcal{H}_V$, then for all $g \in \mathcal{H}_V^o$,

$$|g(x)| \leq M_x \|g\|_{\mathcal{H}_V}.\tag{21}$$

A.2 Proof of Lemma 3.5

$$\begin{aligned}f^{(M)}(x) &= \sum_{m=1}^M \alpha_m k_\theta(x_m, x) \\ &= \sum_{m=1}^M \left(\sum_{V: |V| \leq Q} \theta_V k_V(x_m, x) \right) \\ &= \sum_{V: |V| \leq Q} \theta_V \left(\sum_{m=1}^M k_V(x_m, x) \right) \\ &= \sum_{V: |V| \leq Q} f_V(x).\end{aligned}\tag{22}$$

It remains to show that $f_V \in \mathcal{H}_V^o$. For all $m \in [M]$, $k_V(x_m, \cdot) \in \mathcal{H}_V^o$. Hence, $\theta_V \sum_{m=1}^M k_V(x_m, x) \in \mathcal{H}_V^o$ since \mathcal{H}_V^o is a Hilbert space.

A.3 Proof of Proposition 4.1

We prove the claim using a constructive proof with $p = 2$ variables. Consider the function

$$f(x_1, x_2) = 1 + (x_1 - x_2)^{2k} I(|x_1| \leq M) I(|x_2| \leq M). \quad (23)$$

Suppose the joint distribution of (x_1, x_2) under μ equals

$$\begin{pmatrix} x_1 \\ x_2 \end{pmatrix} \sim N \left(\begin{pmatrix} 0 \\ 0 \end{pmatrix}, \begin{pmatrix} 1 & \rho \\ \rho & 1 \end{pmatrix} \right).$$

Then, the joint distribution of (x_1, x_2) under μ_{\otimes} equals

$$\begin{pmatrix} x_1 \\ x_2 \end{pmatrix} \sim N \left(\begin{pmatrix} 0 \\ 0 \end{pmatrix}, \begin{pmatrix} 1 & 0 \\ 0 & 1 \end{pmatrix} \right).$$

By symmetry,

$$\begin{aligned} \mathbb{E}_{\mu_{\otimes}}[f(x_1, x_2)] &= 2\mu_2(x_2 < 0) \mathbb{E}_{\mu_{\otimes}}[f(x_1, x_2) \mid x_2 < 0] \\ &\geq 2\mu_1(x_1 > c) \mu_2(x_2 < 0) \mathbb{E}_{\mu_{\otimes}}[f(x_1, x_2) \mid x_1 > c, x_2 < 0] \\ &= \mu_1(x_1 > c) \mathbb{E}_{\mu_{\otimes}}[f(x_1, x_2) \mid x_1 > c, x_2 < 0] \\ &\geq \mu_1(x_1 > c) c^{2k} I(|c| < M). \end{aligned} \quad (24)$$

Under μ , we may assume without loss of generality that

$$\begin{aligned} x_1 &\sim \mathcal{N}(0, 1) \\ \epsilon &\sim \mathcal{N}(0, 1) \quad \text{s.t.} \quad \epsilon \perp\!\!\!\perp x_1 \\ x_2 &= \rho x_1 + \sqrt{1 - \rho^2} \epsilon. \end{aligned}$$

Then,

$$\begin{aligned} \lim_{\rho \rightarrow 1} \mathbb{E}_{\mu} f(x_1, x_2) &= 1 + \lim_{\rho \rightarrow 1} \int (x_1 - x_2)^{2k} I(|x_1| \leq M) I(|x_2| \leq M) d\mu(x_1, x_2) \\ &= 1 + \lim_{\rho \rightarrow 1} \int (x_1 - \rho x_1 - \sqrt{1 - \rho^2} \epsilon)^{2k} I(|x_1| \leq M) I(|x_2| \leq M) d\mu_{\otimes}(x_1, \epsilon) \\ &= 1 + \int \lim_{\rho \rightarrow 1} (x_1 - \rho x_1 - \sqrt{1 - \rho^2} \epsilon)^{2k} I(|x_1| \leq M) I(|x_2| \leq M) d\mu_{\otimes}(x_1, \epsilon) \\ &= 1, \end{aligned} \quad (25)$$

where the second to last line follows from the Dominated Convergence Theorem since $f(x_1, x_2)$ is uniformly bounded by $(2M)^{2k}$. Since $\mathbb{E}_\mu f(x_1, x_2) > 1$ for $0 \leq \rho < 1$, there exists a sequence $\{\rho_k\}_{k=1}^\infty$ such that for all $k \in \mathbb{N}$, $1 < \mathbb{E}_{\mu_k} f(x_1, x_2) < 2$ and $0 < \rho_k < 1$, where μ_k sets $\rho = \rho_k$. Pick k' large enough so that $f_{\{\emptyset\}}^{\mu_{\otimes}} > 2$. Then, for $k \geq k'$,

$$\begin{aligned} \frac{|f_{\{\emptyset\}}^{\mu_{\otimes}} - f_{\{\emptyset\}}^{\mu_k}|}{|f_{\{\emptyset\}}^{\mu_k}|} &\geq \frac{|f_{\{\emptyset\}}^{\mu_{\otimes}} - f_{\{\emptyset\}}^{\mu_k}|}{2} \\ &= \frac{f_{\{\emptyset\}}^{\mu_{\otimes}} - f_{\{\emptyset\}}^{\mu_k}}{2} \\ &> \frac{f_{\{\emptyset\}}^{\mu_{\otimes}} - 2}{2} \end{aligned} \tag{26}$$

Let $k^* = \max\left(k', \left\lceil .5 \sqrt{\frac{2(\Delta+1)}{\mu_1(x_1 > c)}} \right\rceil\right)$. Then, by Eq. (24) and Eq. (26), $\frac{|f_{\{\emptyset\}}^{\mu_{\otimes}} - f_{\{\emptyset\}}^{\mu_{k^*}}|}{|f_{\{\emptyset\}}^{\mu_{k^*}}|} > \Delta$.

A.4 Proof of Lemma 3.4

By equation 2.25 of Rasmussen and Williams [2006, Chapter 2], Eq. (6) equals the posterior predictive mean of the following Bayesian model:

$$\begin{aligned} f &\sim GP(0, k_\theta) \\ y \mid f, x &\sim \mathcal{N}(f(x), \sigma_{\text{noise}}^2 = \lambda). \end{aligned}$$

We may re-write k_θ as,

$$\begin{aligned} k_\theta(x, \tilde{x}) &= \sum_{V: |V| \leq Q} \theta_V \Phi_V^T(x) \Phi_V^T(\tilde{x}) \\ &= \sum_{V: |V| \leq Q} \Phi_V^T(x) [\theta_V I_{B^V \times B^V}] \Phi_V^T(\tilde{x}) \\ &= \sum_{V: |V| \leq Q} \Phi_V^T(x) \Sigma_V \Phi_V^T(\tilde{x}), \end{aligned}$$

where $\Sigma_V = \theta_V I_{B^V \times B^V}$. Then, by Rasmussen and Williams [2006, Chapter 2.1.2] and the additive property of kernels, $f \sim GP(0, k_\theta)$ has the same distribution as drawing a set of regression coefficients $\Theta_V \sim \mathcal{N}(0, \Sigma_V)$ and setting $f = \sum_{V: |V| \leq Q} \Theta_V^T \Phi_V(\cdot)$. Hence, the posterior predictive mean of the Gaussian process at a point x equals $\sum_{V: |V| \leq Q} \hat{\Theta}_V^T \Phi_V(x)$.

A.5 Proof of Theorem 3.9

$$\begin{aligned}
k_{\text{SKIM-FA}}(x, \tilde{x}) &= \sum_{V: |V| \leq Q} \left[\eta_{|V|}^2 \prod_{i \in V} \kappa_i^2 \right] k_V(x, \tilde{x}) \\
&= \sum_{V: |V| \leq Q} \left[\eta_{|V|}^2 \prod_{i \in V} \kappa_i^2 \right] \prod_{i \in V} k_i(x_i, \tilde{x}_i) \\
&= \sum_{V: |V| \leq Q} \left[\eta_{|V|}^2 \prod_{i \in V} \kappa_i^2 k_i(x_i, \tilde{x}_i) \right] \\
&= \sum_{q=1}^Q \sum_{V: |V|=q} \left[\eta_{|V|}^2 \prod_{i \in V} \kappa_i^2 k_i(x_i, \tilde{x}_i) \right] \\
&= \sum_{q=1}^Q \eta_q^2 \sum_{V: |V|=q} \left[\prod_{i \in V} \kappa_i^2 k_i(x_i, \tilde{x}_i) \right]
\end{aligned} \tag{27}$$

Let $\tilde{k}_i(\cdot, \cdot) = \kappa_i^2 k_i(\cdot, \cdot)$. Then, Vapnik [1995, pg. 199] shows that

$$\bar{k}_q := \sum_{V: |V|=q} \prod_{i \in V} \tilde{k}_i = \frac{1}{q} \sum_{s=1}^q (-1)^{s+1} \bar{k}_{q-s} k^s, \tag{28}$$

where $k^s(x, \tilde{x}) = \sum_{i=1}^p [\tilde{k}_i(x_i, \tilde{x}_i)]^s$ and $\bar{k}_0(x, \tilde{x}) = 1$. The result follows from Eq. (27) and Eq. (28).

A.6 Proof of Corollary 3.10

Computing and storing $k^1(x, \tilde{x}), \dots, k^Q(x, \tilde{x})$ takes $O(pQ)$ time and requires $O(Q)$ memory, respectively. After computing and storing $\bar{k}_1(x, \tilde{x}), \dots, \bar{k}_q(x, \tilde{x}), \bar{k}_{q+1}(x, \tilde{x})$ takes $O(q+1)$ time. Hence, computing all $\bar{k}_1(x, \tilde{x}), \dots, \bar{k}_Q(x, \tilde{x})$ terms takes $O(Q^2)$ time given $k^1(x, \tilde{x}), \dots, k^Q(x, \tilde{x})$. Since $Q < p$, computing $k_{\text{SKIM-FA}}(x, \tilde{x})$ takes $O(pQ)$ time.

A.7 Proof of Proposition 5.1

$$\begin{aligned}
\frac{\partial L}{\partial \tilde{U}_i^{(t)}} &= \frac{\partial L}{\partial \kappa_i^{(t)}} \frac{\partial \kappa_i}{\partial U_i^{(t)}} \frac{\partial U_i^{(t)}}{\partial \tilde{U}_i^{(t)}} \\
&= \frac{\partial L}{\partial \kappa_i^{(t)}} I(U_i^{(t)} > c) \frac{2\tilde{U}_i^{(t)}}{(\tilde{U}_i^{(t)} + 1)^2}.
\end{aligned}$$

Since $\kappa_i^{(t)} = 0$, that implies $U_i^{(t)} \leq c$. Hence, $\frac{\partial L}{\partial \tilde{U}_i^{(t)}} = 0$. Consequently,

$$\begin{aligned}\tilde{U}_i^{(t+1)} &= \tilde{U}_i^{(t)} - \gamma \frac{\partial L}{\partial \tilde{U}_i^{(t)}} \\ &= \tilde{U}_i^{(t)}.\end{aligned}\tag{29}$$

By Eq. (29), $\kappa_i^{(t')} = 0$ for all $t' \geq t$.

A.8 Proof of Lemma 4.4

It suffices to prove that any $f_V \in \mathcal{H}_V$ is square-integrable with respect to any probability measure. Since ϕ_{ib} is a continuous function on a compact set, there exists a $0 < M_{ib} < \infty$ such that $|\phi_{ib}|$ is bounded by M_{ib} . Without loss of generality, assume $V = \{1, \dots, q\}$. Then, there exists coefficients $c_{b_1, \dots, b_q} \in \mathbb{R}$ such that

$$\begin{aligned}f_V(x_V) &= \sum_{b_1 \in [B_1]} \cdots \sum_{b_q \in [B_q]} c_{b_1, \dots, b_q} \prod_{i=1}^q \phi_{ib_i}(x_i) \\ &\leq \sum_{b_1 \in [B_1]} \cdots \sum_{b_q \in [B_q]} c_{b_1, \dots, b_q} M_*^q \\ &< \infty\end{aligned}$$

for all x_V , where $M_* = \max_{i \in [p]} \max_{b \in [B_i]} M_{ib} < \infty$ since $B_i < \infty$. Hence, for any probability measure μ ,

$$\begin{aligned}\int |f_V(x_V)|^2 d\mu &< \int \left(\sum_{b_1 \in [B_1]} \cdots \sum_{b_q \in [B_q]} c_{b_1, \dots, b_q} M_*^q \right)^2 d\mu \\ &= \left(\sum_{b_1 \in [B_1]} \cdots \sum_{b_q \in [B_q]} c_{b_1, \dots, b_q} M_*^q \right)^2 \\ &< \infty.\end{aligned}\tag{30}$$

A.9 Proof of Theorem 4.5

Let

$$\begin{aligned}
\tilde{f}_{ij} &= f_{\{i,j\}}^{\mu_\otimes} - [\Psi_{ij}^i \Phi_i + \Psi_{ij}^j \Phi_j + \Psi_{ij}^0] \\
\tilde{f}_i &= f_{\{i\}}^{\mu_\otimes} + \sum_{j>i} \Psi_{ij}^i \Phi_i + \sum_{j<i} \Psi_{ji}^i \Phi_i(x_i) \\
\tilde{f}_\emptyset &= f_\emptyset^{\mu_\otimes} + \sum_{i<j} \Psi_{ij}^0.
\end{aligned} \tag{31}$$

We start by proving that $f = \tilde{f}_\emptyset + \sum_{i=1}^p \tilde{f}_i + \sum_{i,j=1}^p \tilde{f}_{ij}$. Expanding each component,

$$\begin{aligned}
\tilde{f}_\emptyset + \sum_i \tilde{f}_i + \sum_{i<j} \tilde{f}_{ij} &= \tilde{f}_\emptyset + \sum_i \tilde{f}_i + \sum_{i<j} [f_{\{i,j\}}^{\mu_\otimes} - [\Psi_{ij}^i \Phi_i + \Psi_{ij}^j \Phi_j + \Psi_{ij}^0]] \\
&= f_\emptyset^{\mu_\otimes} + \sum_i \tilde{f}_i + \sum_{i<j} [f_{\{i,j\}}^{\mu_\otimes} - [\Psi_{ij}^i \Phi_i + \Psi_{ij}^j \Phi_j]] \\
&= f_\emptyset^{\mu_\otimes} + \sum_i \left[f_{\{i\}}^{\mu_\otimes} + \sum_{j>i} \Psi_{ij}^i \Phi_i + \sum_{j<i} \Psi_{ji}^i \Phi_i \right] + \\
&\quad \sum_{i<j} [f_{\{i,j\}}^{\mu_\otimes} - [\Psi_{ij}^i \Phi_i + \Psi_{ij}^j \Phi_j]] \\
&= f_\emptyset^{\mu_\otimes} + \sum_i f_{\{i\}}^{\mu_\otimes} + \sum_{i<j} f_{\{i,j\}}^{\mu_\otimes} + \\
&\quad \sum_i \sum_{j>i} \Psi_{ij}^i \Phi_i + \sum_i \sum_{j<i} \Psi_{ji}^i \Phi_i - \sum_{i<j} [\Psi_{ij}^i \Phi_i + \Psi_{ij}^j \Phi_j] \\
&= f + \sum_i \sum_{j>i} \Psi_{ij}^i \Phi_i + \sum_i \sum_{j<i} \Psi_{ji}^i \Phi_i - \sum_i \sum_{j>i} [\Psi_{ij}^i \Phi_i + \Psi_{ij}^j \Phi_j] \\
&= f + \sum_i \sum_{j<i} \Psi_{ji}^i \Phi_i - \sum_i \sum_{j>i} \Psi_{ij}^j \Phi_j \\
&= f + \sum_i \sum_{j<i} \Psi_{ji}^i \Phi_i - \sum_j \sum_{j<i} \Psi_{ji}^i \Phi_j \\
&= f.
\end{aligned}$$

We now prove that there exists unique coefficients, $\Psi_{ij}^i \in \mathbb{R}^{1 \times B_i}$, $\Psi_{ij}^j \in \mathbb{R}^{1 \times B_j}$, $\Psi_{ij}^0 \in \mathbb{R}$, such that \tilde{f}_{ij} belongs to the orthogonal complement of the Hilbert space $\mathcal{H}_{\{i,j\}}^{\text{add}} := \text{span}\{1, \{\phi_{ib}\}_{b=1}^{B_i}, \{\phi_{jb}\}_{b=1}^{B_j}\} = \mathcal{H}_\emptyset \oplus \mathcal{H}_{\{i\}} \oplus \mathcal{H}_{\{j\}}$. Recall that $\mathcal{H}_{\{i,j\}} = \text{span}\{1, \{\phi_{ib}\}_{b=1}^{B_i}, \{\phi_{jb}\}_{b=1}^{B_j}, \{\phi_{ib}\phi_{jb'}\}_{b \in [B_i], b' \in [B_j]}\}$.

Then, $f_{\{i,j\}}^{\mu_{\otimes}} \in \mathcal{H}_{\{i,j\}}$ and $\mathcal{H}_{\{i,j\}}^{\text{add}}$ is a closed convex subspace of $\mathcal{H}_{\{i,j\}}$. Therefore, by the Hilbert Projection Theorem, there exists unique $\bar{f}_{ij} \in \mathcal{H}_{\{i,j\}}^{\text{add}}$ and $f_{ij}^{\perp} \in \mathcal{H}_{\{i,j\}}$ such that

$$\begin{aligned} f_{\{i,j\}}^{\mu_{\otimes}} &= \bar{f}_{ij} + f_{ij}^{\perp} \quad \text{s.t.} \\ \langle g, f_{ij}^{\perp} \rangle_{\mu} &= 0 \quad \forall g \in \mathcal{H}_{\{i,j\}}^{\text{add}}. \end{aligned} \quad (32)$$

Since $\text{span}\{1, \{\phi_{ib}\}_{b=1}^{B_i}, \{\phi_{jb}\}_{b=1}^{B_j}\}$ is a linearly independent basis of $\mathcal{H}_{\{i,j\}}^{\text{add}}$, there exists unique coefficients, $\Psi_{ij}^i \in \mathbb{R}^{1 \times B_i}, \Psi_{ij}^j \in \mathbb{R}^{1 \times B_j}, \Psi_{ij}^0 \in \mathbb{R}$, such that $\bar{f}_{ij} = \Psi_{ij}^i \Phi_i^T(x_i) + \Psi_{ij}^j \Phi_j^T(x_j) + \Psi_{ij}^0$.

To complete the proof, we need to show that $\tilde{f}_{ij} = f_{\{i,j\}}^{\mu}, \tilde{f}_i = f_{\{i\}}^{\mu}, \tilde{f}_{\emptyset} = f_{\emptyset}^{\mu}$. It suffices to show that

$$\begin{aligned} \int_{x_i} \tilde{f}_i d\mu_i &= 0 \\ \int_{x_i, x_j} \tilde{f}_{ij} d\mu_i &= 0 \\ \int_{x_i, x_j} \tilde{f}_i \tilde{f}_{ij} d\mu(x_i, x_j) &= 0. \end{aligned} \quad (33)$$

The last two equalities in Eq. (33) follow directly from Eq. (32). For the first equality in Eq. (33), notice that

$$\begin{aligned} \int_{x_i} \tilde{f}_i d\mu_i &= \mathbb{E}_{\mu_i} \tilde{f}_i \\ &= \mathbb{E}_{\mu_i} \left[f_{\{i\}}^{\mu_{\otimes}} + \sum_{j>i} \Psi_{ij}^i \Phi_i + \sum_{j<i} \Psi_{ji}^i \Phi_i \right] \\ &= \mathbb{E}_{\mu_i} f_{\{i\}}^{\mu_{\otimes}} + \sum_{j>i} \mathbb{E}_{\mu_i} [\Psi_{ij}^i \Phi_i] + \sum_{j<i} \mathbb{E}_{\mu_i} [\Psi_{ji}^i \Phi_i] \\ &= \sum_{j>i} \Psi_{ij}^i \mathbb{E}_{\mu_i} [\Phi_i] + \sum_{j<i} \Psi_{ji}^i \mathbb{E}_{\mu_i} [\Phi_i] \\ &= 0, \end{aligned}$$

where the last equation follows from the fact that the components of Φ_i span $\mathcal{H}_{\{i\}}^o$ (and hence are all zero mean).

A.10 Proof of Proposition 5.2

As shown in the proof of Theorem 4.5, $\Psi_{ij}^i \in \mathbb{R}^{1 \times B_i}, \Psi_{ij}^j \in \mathbb{R}^{1 \times B_j}, \Psi_{ij}^0 \in \mathbb{R}$ equal the unique set of coefficients such that $\bar{f}_{ij} = \Psi_{ij}^i \Phi_i + \Psi_{ij}^j \Phi_j + \Psi_{ij}^0$ for \bar{f}_{ij} defined in Eq. (32) and also shown

below:

$$\begin{aligned} f_{\{i,j\}}^{\mu_{\otimes}} &= \bar{f}_{ij} + f_{ij}^{\perp} \quad \text{s.t.} \\ \langle g, f_{ij}^{\perp} \rangle_{\mu} &= 0 \quad \forall g \in \mathcal{H}_{\{i,j\}}^{\text{add}}. \end{aligned}$$

Let $y_{ij}^{(w)} = f_{\{i,j\}}^{\mu_{\otimes}}(x_i^{(w)}, x_j^{(w)})$ and $\epsilon_{ij}^{(w)} = f_{ij}^{\perp}(x_i^{(w)}, x_j^{(w)})$, where $x^{(w)} \stackrel{\text{iid}}{\sim} \mu$. Then,

$$y_{ij}^{(w)} = \Psi_{ij}^i \Phi_i(x_i^{(w)}) + \Psi_{ij}^j \Phi_j(x_j^{(w)}) + \Psi_{ij}^0 + \epsilon_{ij}^{(w)} \quad x^{(w)} \stackrel{\text{iid}}{\sim} \mu. \quad (34)$$

Then, Eq. (34) is a special case of the random design linear model under misspecification studied in Hsu et al. [2014]. Hence, by Hsu et al. [2014, Theorem 11] we can consistently recover Ψ_{ij}^i , Ψ_{ij}^j , Ψ_{ij}^0 by using ordinary least-squares. Hence Algorithm 4 recovers Ψ_{ij}^i , Ψ_{ij}^j , Ψ_{ij}^0 as $W \rightarrow \infty$.

B Literature Review

Finite Basis Expansion Methods. Stone [1994] introduced the hierarchical functional decomposition and derived statistical rates of convergence by approximating \mathcal{H} using a finite B-spline tensor product basis. Huang [1998] later extended this result to general tensor product families such as wavelets, polynomials, etc. There have been a number of specific Bayesian and frequentist methods that fall within the general class of models described in Huang [1998]; see, for example, Wei et al. [2019], Scheipl et al. [2012], Curtis et al. [2014], Ferrari and Dunson [2020b]. Unfortunately, since these methods explicitly generate the tensor product basis, they are computationally intractable as p increases beyond a few hundred or thousand covariates.

Linear models trivially fall within this class as well. For $Q = 1$, the Lasso and the many related techniques provide fast variable selection and estimation in high-dimensional linear models [Chen et al., 1998, Candes and Tao, 2007, Nakagawa et al., 2016]. For $Q = 2$, the hierarchical Lasso [Bien et al., 2013] extends the Lasso to model interactions, and there have been many variants of this model; see, for example, Lim and Hastie [2015], Shah [2016]. However, these methods take at least $O(p^2)$ time since they explicitly model all main and interaction effects. Other linear interaction methods assume that the interactions have a low-rank structure. This structure helps both statistically and computationally; see, for example, Rendle [2010], Ferrari and Dunson [2020a]. However, this low-rank structure in the interaction effects might not always

hold in practice.

Two-Stage & Forward-Stage Approaches. Instead of modeling interactions jointly, a common heuristic (similar in spirit to forward stepwise regression) is greedily adding interactions such as in multivariate additive regression splines (MARS) or GA2M [Lou et al., 2013]. Another common approach is performing computationally cheap variable selection methods designed for generalized additive models (e.g., Lasso or SpAM [Liu et al., 2008]) to identify a sparse set of relevant variables. By restricting to a small set of variables, one can then apply more computationally intensive interactions techniques such as RKHS ANOVA methods.

Either of the two approaches above requires some form of strong-hierarchy, namely that all interactions have non-zero main effects, to consistently identify the correct set of variables. While some problems have strong main effects, in other applications this may not be the case. For example, in genome-wide associate studies, fitting an additive-only model to predict an individual’s height from genetics only has an R^2 of about 5% even though height is well-predicted by parents’ heights (thought to be between 80% – 90%) [Maher, 2008]. This discrepancy, more generally called the problem of *missing heritability*, remains an open challenge in biology for understanding complex diseases based on genetics. One explanation for missing heritability is not modeling genetic interactions [Maher, 2008, Aschard, 2016, Slim et al., 2018, Greene et al., 2010]. In other words, the main effects might be weak, or in the extreme case some genes might only have interaction effects. Hence, from a purely variable selection standpoint, modeling interactions could help better identify genes that are risk-factors for certain diseases.

In the orthogonal μ case, the statistical benefit from modeling interactions can be easily seen from the decomposition in Eq. (4). Suppose $Q = 2$ and that main effects total signal variance equals 5, the pairwise signal variance equals 90, and the noise variance equals 5. Then, the R^2 for an additive-only model is 5% while the R^2 for interaction model is 90%. Since the achievable signal increases (and necessarily the effective noise variance decreases), performing variable selection in a lower signal-to-noise regime might offset the statistical price of modeling more parameters.

C Zero Mean Kernels and Finite-Basis Functions

In this section, we show how we construct k_i , i.e., the reproducing kernel for $\mathcal{H}_{\{i\}}^o$. We construct k_i by first generating a finite-dimensional basis for $\mathcal{H}_{\{i\}}$. Then, we normalize each basis function to be zero mean and unit variance so that the normalized basis functions span $\mathcal{H}_{\{i\}}^o$. For a more general approach to construct zero mean kernels (e.g., even when $\mathcal{H}_{\{i\}}$ is infinite-dimensional) see Durrande et al. [2013].

Construction. For each covariate dimension i , consider a set of linearly independent basis functions $\{\phi_{ib}\}_{b=1}^{B_i}$ such that

$$\mathcal{H}_{\{i\}} = \text{span}\{1, \phi_{i1}, \dots, \phi_{iB_i}\}.$$

Let $\tilde{\phi}_{ib} = \frac{\phi_{ib} - \mathbb{E}_\mu[\phi_{ib}]}{\sqrt{\text{Var}_\mu[\phi_{ib}]}}$. Then,

$$\mathcal{H}_{\{i\}}^o = \text{span}\{\tilde{\phi}_{i1}, \dots, \tilde{\phi}_{iB_i}\}, \quad \Phi_i := [\tilde{\phi}_{i1}, \dots, \tilde{\phi}_{iB_i}].$$

Hence, $k_i(x_i, \tilde{x}_i) = \Phi_i(x_i)^T \Phi_i(\tilde{x}_i)$ is the reproducing kernel for \mathcal{H}_i^o . In many instances, we do not actually know the joint distribution of the covariates. In this case, we approximate μ with the empirical distribution $\hat{\mu}$ of the datapoints:

$$\begin{aligned} \tilde{\phi}_{ib} &= \frac{\phi_{ib} - \mathbb{E}_{\hat{\mu}}[\phi_{ib}]}{\sqrt{\text{Var}_{\hat{\mu}}[\phi_{ib}]}} \quad \text{s.t.} \\ \hat{\mu} &= \frac{1}{N} \sum_{n=1}^N \delta_{x^{(n)}} \\ \mathbb{E}_{\hat{\mu}}[\phi_{ib}] &= \frac{1}{N} \sum_{n=1}^N \phi_{ib}(x_i^{(n)}) \\ \text{Var}_{\hat{\mu}}[\phi_{ib}] &= \frac{1}{N} \sum_{n=1}^N \phi_{ib}^2(x_i^{(n)}) - \mathbb{E}_{\hat{\mu}}[\phi_{ib}]. \end{aligned}$$

D Additional Algorithmic Details

To fit SKIM-FA, we set the number of iterations $T = 2000$, learning rate $\gamma = 0.1$, and cross-validation batch size $M = 0.2N$ in Algorithm 1. We let the truncation level c in Algorithm 1

depend on the iteration number t for $1 \leq t \leq T$. Empirically, we find gradually increasing c as a function of t works well for accurately selecting the correct covariates and inducing sparsity in κ . We suggest the following schedule for c :

Algorithm 5 Scheduler for Truncation Level c

```

1: procedure TRUNC_SCHEDULER( $U^{(t)}, c_{t-1}, t, r = .001$ )
2:   if  $t < 500$  then return 0
3:   end if
4:   if  $t = 500$  then return  $q_{25}(U_1^{(t)}, \dots, U_p^{(t)}) \triangleright$  Take the 25th% of the components in  $U^{(t)}$ 
5:   end if
   return  $\max(\min((1+r)c_{t-1}, 0.75), c_{t-1})$ 
6: end procedure

```

When $t < 500$, $c = 0$ in Algorithm 5. Hence, since $\kappa_i^{(t)} = \max(U_i^{(t)} - c, 0)$, $\kappa_i^{(t)} \neq 0$ for $t \leq 500$. At iteration 500, we drop the bottom 25th% of covariates (determined by their importance measure $U_i^{(t)}$). Hence, $\kappa^{(500)}$ has 25% of its entries equal to zero. For subsequent iterations, we take the previous truncation level c_t and increase that level by a factor of $(1+r)$ until c_t reaches 0.75. If c_{t-1} is larger than 0.75, we set c_t equal to c_{t-1} .

E MARS ANOVA Procedure

We show how to perform the functional ANOVA decomposition of \hat{f} with respect to $\hat{\mu}_\otimes = \hat{\mu}_1 \otimes \dots \otimes \hat{\mu}_p$, where \hat{f} denotes the regression function fit from MARS and μ_i the empirical distribution of covariate i : $\hat{\mu}_i = \frac{1}{N} \sum_{n=1}^N \delta_{x_i^{(n)}}$. Under $\hat{\mu}_\otimes$, the functional ANOVA decomposition of \hat{f} equals

$$\begin{aligned}
\hat{f}_\emptyset &= \mathbb{E}_{\hat{\mu}_\otimes}[\hat{f}] \\
\hat{f}_{\{i\}}(x_i) &= \mathbb{E}_{\hat{\mu}_\otimes}[\hat{f} \mid x_i = x_i] - \hat{f}_\emptyset \\
\hat{f}_{\{i,j\}}(x_i, x_j) &= \mathbb{E}_{\hat{\mu}_\otimes}[\hat{f} \mid x_i = x_i, x_j = x_j] - \hat{f}_{\{i\}}(x_i) - \hat{f}_{\{j\}}(x_j) - \hat{f}_\emptyset,
\end{aligned} \tag{35}$$

which is also shown in Durrande et al. [2013, Equation 5]. We show how to compute each of the expectations in Eq. (35). The intercept \hat{f}_\emptyset equals the sample average of the fitted values (i.e., \hat{f}

applied to each of the N training datapoints). Let X denote the $N \times p$ matrix of training data. Let X^i equal the matrix obtained by setting all values in the i th column of X equal to x_i and the remaining columns unchanged. Then,

$$\mathbb{E}_{\hat{\mu}_{\otimes}}[\hat{f} \mid x_i = x_i] = \frac{1}{N} \sum_{n=1}^N \hat{f}(X_n^i),$$

where X_n^i is the n th row of X_n^i . Similarly, let X^{ij} equal the matrix obtained by setting all values in the i th and j th columns of X equal to x_i and x_j respectively, and the remaining columns unchanged. Then,

$$\mathbb{E}_{\hat{\mu}_{\otimes}}[\hat{f} \mid x_i = x_i, x_j = x_j] = \frac{1}{N} \sum_{n=1}^N \hat{f}(X_n^{ij}).$$

F Additional Experimental Results

Table F.1: Variable Selection Performance for Main Effects Only Setting.

Method	# Covariates	# Correct Selected	# Wrong Selected	# Correct Not Selected
HierLasso	250	4	0	1
SKIM -FA	250	4	0	1
Pairs Lasso	250	4	5	1
SPAM-2Stage	250	5	52	0
MARS	250	5	58	0
SKIM-FA	500	5	13	0
SPAM-2Stage	500	5	28	0
Pairs Lasso	500	4	39	1
HierLasso	500	4	48	1
MARS	500	5	64	0
SKIM-FA	1000	3	0	2
HierLasso	1000	4	5	1
Pairs Lasso	1000	4	6	1
SPAM-2Stage	1000	5	15	0
MARS	1000	5	70	0

Table F.2: Estimation Performance for Main Effects Only Setting.

Method	p	Correct		Wrong		Correct		Wrong		Total SSE	
		Selected	Not Selected	Selected	Not Selected	Selected	Not Selected	Selected	Not Selected	Total	÷ Signal Variance
		SSE (Main)	SSE (Main)	SSE (Main)	SSE (Main)	SSE (Pair)	SSE (Pair)	SSE (Pair)	SSE (Pair)	SSE	
MARS-EMP	250	0.31	0.00	2.11	0.00	0.00	0.00	2.24	4.66	0.23	
SPAM-2Stage	250	2.77	0.00	1.99	0.00	0.00	0.00	0.08	4.84	0.24	
SKIM-FA	250	2.75	4.02	0.00	0.00	0.00	0.00	0.39	7.16	0.36	
MARS-VANILLA	250	73.17	0.00	2.37	0.00	0.00	0.00	9.89	85.43	4.27	
SPAM-2Stage	500	2.82	0.00	1.25	0.00	0.00	0.00	0.04	4.11	0.21	
SKIM-FA	500	2.75	0.00	0.49	0.00	0.00	0.00	1.40	4.64	0.23	
MARS-EMP	500	0.38	0.00	2.37	0.00	0.00	0.00	2.19	4.95	0.25	
MARS-VANILLA	500	35.67	0.00	3.62	0.00	0.00	0.00	9.22	48.51	2.43	
SPAM-2Stage	1000	2.67	0.00	0.78	0.00	0.00	0.00	0.02	3.46	0.17	
MARS-EMP	1000	0.45	0.00	2.68	0.00	0.00	0.00	2.39	5.51	0.28	
SKIM-FA	1000	2.70	8.10	0.00	0.00	0.00	0.00	0.24	11.03	0.55	
MARS-VANILLA	1000	16.14	0.00	1.56	0.00	0.00	0.00	10.33	28.02	1.40	

Table F.3: Variable Selection Performance for Equal Main and Interaction Effects Setting.

Method	# of Covariates	# Correct Selected	# Wrong Selected	# Correct Not Selected
SKIM-FA	250	5	1	0
HierLasso	250	5	25	0
SPAM-2Stage	250	5	37	0
MARS	250	5	84	0
Pairs Lasso	250	5	89	0
SKIM-FA	500	5	0	0
SPAM-2Stage	500	5	29	0
HierLasso	500	5	30	0
MARS	500	5	69	0
Pairs Lasso	500	5	182	0
SKIM-FA	1000	5	0	0
SPAM-2Stage	1000	5	15	0
HierLasso	1000	5	40	0
MARS	1000	5	71	0
Pairs Lasso	1000	5	213	0

Table F.4: Estimation Performance for Equal Main and Interaction Effects Setting.

Method	p	Correct		Wrong		Correct		Wrong		Total SSE	
		Selected	Not Selected	Selected	Not Selected	Selected	Not Selected	Selected	Not Selected	Total	÷ Signal Variance
		SSE (Main)	SSE (Main)	SSE (Main)	SSE (Main)	SSE (Pair)	SSE (Pair)	SSE (Pair)	SSE (Pair)	SSE	
SKIM-FA	250	1.62	0.00	0.08	0.52	0.00	0.00	0.17	2.39	0.12	
SPAM-2Stage	250	1.63	0.00	1.72	8.84	0.00	0.00	0.11	12.30	0.62	
MARS-EMP	250	0.71	0.00	4.44	2.17	0.00	0.00	5.69	13.01	0.65	
MARS-VANILLA	250	24.91	0.00	5.28	17.13	0.00	0.00	18.03	65.35	3.27	
SKIM-FA	500	1.52	0.00	0.00	0.41	0.00	0.00	0.00	1.93	0.10	
SPAM-2Stage	500	1.62	0.00	3.74	2.16	0.00	0.00	5.47	12.99	0.65	
MARS-EMP	500	0.71	0.00	4.69	1.63	0.96	0.96	6.57	14.56	0.73	
MARS-VANILLA	500	11.36	0.00	13.22	15.62	0.96	0.96	23.55	64.71	3.24	
SKIM-FA	1000	1.54	0.00	0.00	0.29	0.00	0.00	0.00	1.82	0.09	
SPAM-2Stage	1000	1.67	0.00	1.07	0.41	0.00	0.00	2.16	5.31	0.27	
MARS-EMP	1000	0.61	0.00	3.84	1.70	0.00	0.00	2.52	8.67	0.43	
MARS-VANILLA	1000	454.88	0.00	3.16	21.46	0.00	0.00	13.22	492.72	24.64	

Table F.5: Variable Selection Performance for Weak Main Effects Setting.

Method	# Covariates	# Correct Selected	# Wrong Selected	# Correct Not Selected
SKIM-FA	250	5	6	0
MARS	250	5	75	0
SPAM-2Stage	250	4	77	1
Pairs Lasso	250	5	123	0
HierLasso	250	5	160	0
SKIM-FA	500	5	16	0
SPAM-2Stage	500	1	21	4
HierLasso	500	5	62	0
Pairs Lasso	500	5	85	0
MARS	500	2	132	3
SKIM-FA	1000	5	9	0
SPAM-2Stage	1000	1	41	4
MARS	1000	5	75	0
HierLasso	1000	5	120	0
Pairs Lasso	1000	5	144	0

Table F.6: Estimation Performance for Weak Main Effects Setting.

Method	p	Correct		Wrong		Correct		Wrong		Total SSE	
		Selected SSE (Main)	Not Selected SSE (Main)	Selected SSE (Main)	Correct Selected SSE (Pair)	Not Selected SSE (Pair)	Selected SSE (Pair)	Total SSE	÷ Signal Variance		
SKIM-FA	250	0.45	0.00	0.95	0.73	0.00	0.77	2.89	0.14		
MARS-EMP	250	1.46	0.00	4.02	4.83	0.00	4.67	14.97	0.75		
SPAM-2Stage	250	0.09	0.05	2.22	10.72	7.73	0.42	21.23	1.06		
MARS-VANILLA	250	22497.35	0.00	7.31	148073.29	0.00	18.55	170596.50	8529.83		
SKIM-FA	500	0.69	0.00	2.05	1.50	0.00	1.37	5.61	0.28		
SPAM-2Stage	500	0.27	0.20	4.09	0.00	19.46	0.08	24.11	1.21		
MARS-EMP	500	0.41	0.15	21.92	0.00	19.46	15.56	57.51	2.88		
MARS-VANILLA	500	0.10	0.15	323788.65	0.00	19.46	324588.33	648396.70	32419.83		
SKIM-FA	1000	0.72	0.00	1.37	0.61	0.00	0.63	3.33	0.17		
MARS-EMP	1000	0.67	0.00	5.86	3.37	0.00	5.63	15.52	0.78		
SPAM-2Stage	1000	0.16	0.20	6.69	0.00	18.33	0.31	25.69	1.28		
MARS-VANILLA	1000	23.62	0.00	3.18	23.16	0.00	15.43	65.39	3.27		

Table F.7: Proxy Ground Truth Effects and Signal Variances for the Bike Sharing Dataset.

Effect	Signal Variance
Hour	0.382
Air Temp.	0.104
Humidity	0.024
Windspeed	0.002
Hour x Air Temp.	0.047
Hour x Humidity	0.01
Hour x Windspeed	0.002
Air Temp. x Humidity	0.012
Air Temp. x Windspeed	0.005
Humidity x Windspeed	0.003

F.1 Appending Irrelevant but Real Covariates to the Bike Sharing Dataset

In Section 7, we appended fake covariates drawn from a $\text{Uniform}(0, 1)$ distribution to the Bike Sharing Dataset for various choices of p_{noise} . In many applications, however, covariates are correlated and this correlation structure might affect the performance of a method. To create a design matrix with a non-trivial correlation structure, we start by taking a completely different dataset, namely the SECOM dataset from the UCI Machine Learning repository which contains 591 covariates related to semi-conductor manufacturing.⁷ Then, we append these covariates to the Bike Sharing dataset. Since these two datasets are independent, the covariates in the SECOM dataset play the same role as the synthetic fake covariates in Section 7 (i.e., should not be selected) but now have a real correlation structure. Table F.10 and Table F.11 summarize how each method performs in terms of variable selection and estimation, respectively.

⁷We only consider 432 continuous covariates (with non-zero variance) in the SECOM dataset.

Table F.8: Variable Selection Performance for the Bike Sharing Dataset.

Method	# Covariates	# Original Selected	# Wrong Selected
SKIM-FA	250	2	0
HierLasso	250	3	7
Pairs Lasso	250	3	29
MARS	250	3	96
SPAM-2Stage	250	4	97
SKIM-FA	500	2	0
HierLasso	500	3	8
SPAM-2Stage	500	3	22
Pairs Lasso	500	3	39
MARS	500	4	109
SKIM-FA	1000	3	0
HierLasso	1000	3	5
SPAM-2Stage	1000	3	8
Pairs Lasso	1000	3	76
MARS	1000	3	119

Table F.9: Estimation Performance for the Bike Sharing Dataset.

Method	# Noise	Correct Selected SSE (Main)	Correct Not Selected SSE (Main)	Wrong Selected SSE (Main)	Correct Selected SSE (Pair)	Correct Not Selected SSE (Pair)	Wrong Selected SSE (Pair)	Total SSE
SKIM-FA	250	0.15	0.027	0	0.019	0.038	0	0.233
SPAM-2Stage	250	0.149	0	0.172	0.091	0	0.01	0.422
MARS-EMP	250	0.209	0.002	0.476	0.052	0.026	0.344	1.11
MARS-Vanilla	250	6.522	0.002	1.644	1.036	0.026	2.2	11.431
SKIM-FA	500	0.148	0.027	0	0.019	0.038	0	0.231
SPAM-2Stage	500	0.15	0.002	0.057	0.081	0.009	0.002	0.302
MARS-EMP	500	0.225	0	0.529	0.052	0.026	0.3	1.131
MARS-Vanilla	500	5.564	0	0.5	1.037	0.026	2.085	9.212
SKIM-FA	1000	0.145	0.002	0	0.107	0.009	0	0.263
SPAM-2Stage	1000	0.149	0.002	0.027	0.081	0.009	0.000	0.269
MARS-EMP	1000	0.214	0.002	0.485	0.054	0.026	0.245	1.026
MARS-Vanilla	1000	6.556	0.002	0.796	0.947	0.026	1.882	10.209

Table F.10: Variable Selection Performance for the Bike Sharing-SECOM Dataset.

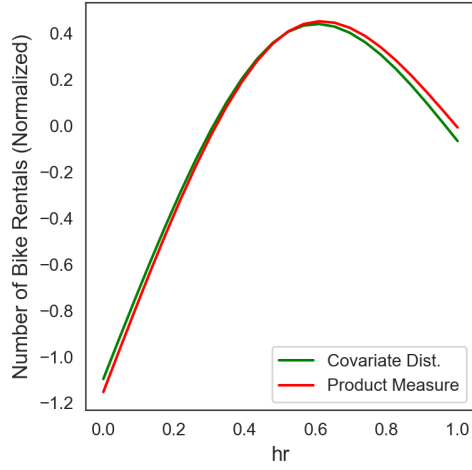
Method	# Covariates	# Original Selected	# Wrong Selected
SKIM-FA	432	2	0
HierLasso	432	3	1
SPAM-2Stage	432	0	0
Pairs Lasso	432	3	14
MARS	432	3	97

Table F.11: Estimation Performance for the Bike Sharing-SECOM Dataset.

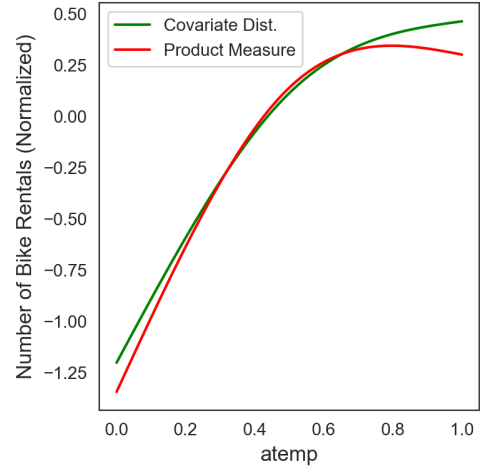
Method	# Noise	Correct Selected SSE (Main)	Correct Not Selected SSE (Main)	Wrong Selected SSE (Main)	Correct Selected SSE (Pair)	Correct Not Selected SSE (Pair)	Wrong Selected SSE (Pair)	Total SSE
SKIM-FA	432	0.137	0.026	0	0.016	0.029	0	0.208
SPAM-2Stage	432	0	0.549	0	0	0.074	0	0.623
MARS-EMP	432	0.212	0.001	7.416	0.049	0.018	6.113	13.810
MARS-Vanilla	432	3.876	0.001	85.369	1.704	0.0178	104.405	195.373

F.2 Impact of Correlated Predictors on the Functional ANOVA for the Bike Sharing Dataset

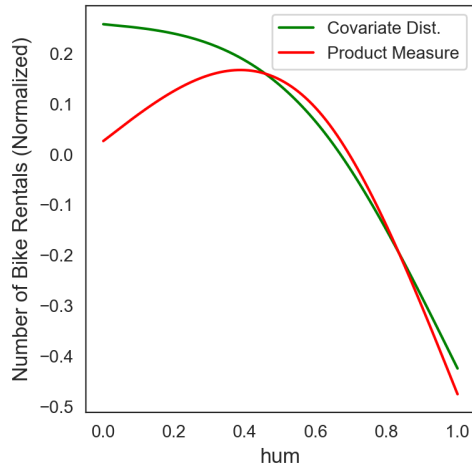
We perform the same analysis as in Section 7.5 but for the Bike Sharing dataset in Fig. F.1. Unlike the Concrete Compressive Strength dataset, however, we do not see a large difference between the two functional ANOVA decompositions for the Bike Sharing dataset in Fig. F.1.



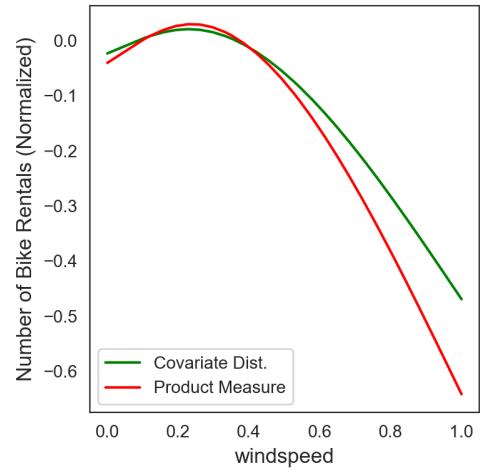
(a) Main Effect of Hour of the Day on Rentals



(b) Main Effect of Hour of Temperature



(c) Main Effect of Humidity



(d) Main Effect of Windspeed

Figure F.1: Effect of Correlated Predictors on the Bike Sharing Dataset